Conductive Nanomaterials for Printed Electronics

*Alexander Kamyshny and Shlomo Magdassi**

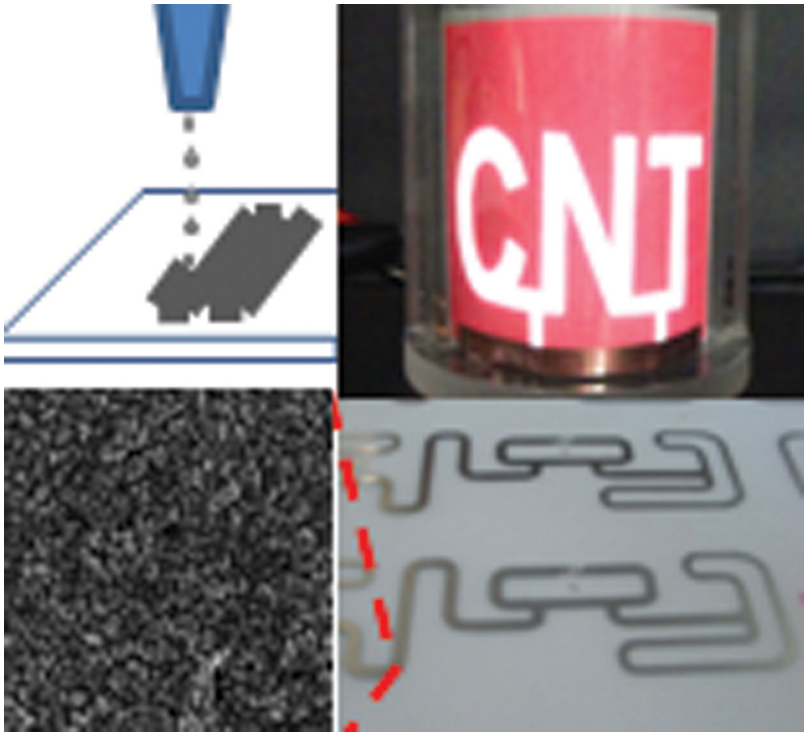

From the Contents

This is a review on recent developments in the field of conductive nanomaterials and their application in printed electronics, with particular emphasis on inkjet printing of ink formulations based on metal nanoparticles, carbon nanotubes, and graphene sheets. The review describes the basic properties of conductive nanomaterials suitable for printed electronics (metal nanoparticles, carbon nanotubes, and graphene), their stabilization in dispersions, formulations of conductive inks, and obtaining conductive patterns by using various sintering methods. Applications of conductive nanomaterials for electronic devices (transparent electrodes, metallization of solar cells, RFID antennas, TFTs, and light emitting devices) are also briefly reviewed.

1. Introduction

In the past decade, a tremendous interest in printed electronics had become evident.[1–8] Printed electronics refers to the application of printing technologies for the fabrication of electronic circuits and devices. Especially important is the manufacturing of such devices on flexible (bendable plastic or paper) substrates (the term "flexible electronics" is often used in this case). Traditionally, electronic devices are mainly manufactured by photolithography, vacuum deposition, and electroless plating processes. All these methods are multistaged, require high-cost equipment and the use of environmentally undesirable chemicals which result usually in the formation large amounts of waste. However, the market of printed electronics, which is estimated to exceed $300 billion over the next 20 years,[3] requires manufacturing techniques that are faster, cheaper and eco-friendlier compared to traditional production methods. In this regard, additive inkjet printing, which is a non-impact, dot-matrix digital patterning technique, is a very attractive technology for direct metallization. This is important for manufacturing printed circuit boards, RFID tags, thin film transistors, light emitting devices, solar cells, transparent electrodes, touch screens, and flexible displays.[1,3–6,8–11] Inkjet printing is favorable for automation and enables patterning with high resolution: line and space dimensions can be as small as 20 μm.[6,12] In addition, inkjet printing is very suitable for manufacturing large area plastic electronics by the roll-to-roll (R2R) technique.

All inkjet technologies are based on digitally controlled generation and ejection of drops of liquid inks with typical diameters of 50–80 μm, from a printhead nozzle onto a substrate. This is realized by two different modes of operation: continuous (CIJ) and drop-on-demand (DOD) printing.[12–14] Today, the majority of inkjet printers are based on the DOD technology, mainly with piezoelectric or thermal generation of ink droplets, which are jetted onto a specified position on a substrate.

Conductive inkjet ink is a multi-component system that contains a conducting material in a liquid vehicle (aqueous or organic) and various additives (such as rheology and surface tension modifiers, humectants, binders and defoamers) that enable optimal performance of the whole system, including the printing device and the substrate.[1,6,12] The conductive material may be dispersed nanoparticles (NPs), a dissolved organometallic compound, or a conductive polymer (both, dissolved and dispersed).[1,2,6] The choice of the conductive material is mainly determined by the required physical properties of the printed pattern, such as conductivity, optical transparency, stability to bending, and adhesion (especially important for flexible electronics), by the physicochemical properties of the ink, such as aggregation and stability, and by its compatibility with the printing device.

In this review we will focus on the dispersions of conductive nanomaterials, which are usually defined as particles with at least one dimension in the range of 1–100 nm.[15] As a general rule, the size of the particles in inkjet ink formulation should be less than 0.1–0.01 of the diameter of the printhead's orifice to avoid its clogging and blockage. However, the smaller the particles, the better, and an average particle size of 30–50 nm is preferable.[9,16]

One type of nanomaterials to be considered here is metal NPs. Modern wet chemical methods enable large scale production of dispersions of metal NPs, which meet the requirements for inkjet ink formulations, and are suitable for conductive printing.[15] For example, nanosilver inks, which are widely used today for conductive printing, enable obtaining printed patterns with high conductivity which is comparable with that of bulk metal.[1,4,6,9,17–20]

Another family of nanomaterials for conductive printing is carbon-based nanomaterials: carbon nanotubes (CNTs) and graphene. CNTs and graphene sheets are very promising in flexible electronics due to their unique properties, such as high intrinsic current mobility and conductivity, mechanical flexibility, and their potential for low-cost production.[8] Inkjet printing of CNTs and graphene was demonstrated for the fabrication of various electronic devices,[8,10,21–24] and important advantage of such inks is obtaining conductive coatings with high optical transparency.[8,23,24]

The review will focus on synthesis of metal NPs, preparation of stable dispersions of metal NPs, CNTs and graphene sheets, ink formulations based on these dispersions, sintering of metallic printed patterns for obtaining high electrical conductivity, and recent progress in the utilization of metal NPs, CNTs, and graphene for the fabrication of various functional devices.

2. Printable Dispersions of Conductive Nanomaterials: Requirements and Challenges

Applying inkjet techniques to the deposition of functional materials requires the formulation of suitable inks. The basic requirements for conductive inkjet inks are similar to those of graphic art inkjet inks: the ink should demonstrate good printability, good adhesion to specific substrates, high resolution, minimum printer maintenance, and long shelf life. Therefore, important properties such as viscosity, surface tension, wettability and adhesion to substrate should be adjusted to provide optimal printing performance.[12,25] For example, in the case of piezoelectric print heads, the ink viscosity should be in the range of 8–15 cP, while thermal print heads require viscosity below 3 cP.[12]

There are several challenges which should be overcome while using conductive NPs as the functional component of conductive inks. First, NPs in the ink should be stable against aggregation and precipitation in order to provide reproducible performance. Therefore, addition of a stabilizing agent, which is usually a polymeric material or a surfactant, is required. This stabilizer is especially important for

A. Kamyshny, S. Magdassi
Casali Center of Applied Chemistry
Institute of Chemistry
The Center for Nanoscience and Nanotechnology
The Hebrew University of Jerusalem
91904, Jerusalem, Israel
E-mail: magdassi@cc.huji.ac.il

DOI: 10.1002/smll.201303000

NANO MICRO small

dispersions with high metal loading, 20–60 wt%, which are required for obtaining printed patterns with high density of metal to provide high conductivities. However, as will be discussed later, the presence of this stabilizer usually poses a major problem when aiming at high conductivity.

Furthermore, NPs-based conductive inks should provide good electrical conductivity of printed patterns. It is obvious that the best candidates for conductive material are the highly conductive metals, such as Ag ($\sigma = 6.3 \cdot 10^7\ \Omega^{-1}\cdot m^{-1}$), Cu ($\sigma = 5.96 \cdot 10^7\ \Omega^{-1}\cdot m^{-1}$), Au ($\sigma = 4.42 \cdot 10^7\ \Omega^{-1}\cdot m^{-1}$), and Al ($\sigma = 3.78 \cdot 10^7\ \Omega^{-1}\cdot m^{-1}$). Currently, silver is the most reported material for conductive ink, and also the most utilized in industrial applications. Due to their high cost, a major challenge in this field is to replace silver and other noble metals with cheaper ones, such as copper and aluminum. This would depend on the success in avoiding their oxidation at ambient conditions, otherwise an inert atmosphere would be required.[1,26] For example, aluminum undergoes rapid oxidation in air (within ~100 picoseconds) forming a dense thin amorphous Al_2O_3 layer with a thickness of 2–6 nm,[27,28] which results in the loss of electrical conductivity and makes aluminum NPs inapplicable for conductive ink formulations. Oxidation of copper NPs is less rapid, as compared to aluminum, especially in the presence of an excess of a reducing agent.[29] This enables to obtain copper NPs with long-term stability by coating them with a dense layer of capping agent (alkanethiols, long chain fatty acids, polymers)[30–35] or with an air stable metal[26,29] in order to minimize or to prevent the penetration of oxygen to the surface of the NPs.

Another challenge in using metallic nanoparticles is the need for a post-printing process in order to sinter the NPs for obtaining continuous metallic phase, with numerous percolation paths between metal particles within the printed patterns. This is usually an obligatory stage, since the presence of stabilizing agents and other ink components prevents close electrical contacts of NPs due to the existence of insulating organic layers that surround the NPs. The conventional approach for sintering metallic NPs is heating. However, in the case of heat-sensitive substrates (e.g. paper, plastics), heating at temperatures above 120–150 °C is not applicable and, therefore, non-destructive methods of sintering are required.

As to CNT- and graphene-based conductive inks, they can provide a good alternative to metal NPs. Due to their advantageous electrical, optical, and mechanical properties, graphene and CNTs are an attractive material for nanoelectronics and optoelectronics.[3,6,8,10,22,23,36] The intrinsic electrical conductivity of individual CNTs is close to the conductivities of metals.[36] However, because of their large aspect ratio, van der Waals forces cause them to stick together, thus forming large bundles or ropes.[6,36,37] The formation of such large bundles would cause clogging of the printhead nozzles,[6] and the presence of large nanometric tubes would increase the viscosity of the ink, much beyond that which is required for inkjet printing. As for metallic inks, high conductivity of the printed patterns is important for the utilization of CNTs in printed electronics. However, it has been reported that for aggregated CNTs, electric current flows only on the outermost tubes in the bundle, while the inner tubes do not contribute significantly to the current.[36,38] Therefore, the major challenge in formulating conductive inks is the preparation of dispersions composed of separated CNTs without chemical modification, mechanical damage (e.g. buckling, bending) and changes in chirality, which are important for high electrical conductivity.[39–41]

A number of challenges has also to be overcome for large-scale production of graphene printed films for practical application. First, dispersions of graphene have strong tendency to aggregation of graphene layers because of strong inter-sheet van der Waals forces. To overcome this problem, the surface of graphene sheets should be tailored according to the dispersing solvent.[42,43] Second, the graphene concentration in dispersions is usually low <0.01 wt%), and tens of printed layers are required to obtain films with a proper functionality.[22,44] In addition, most studies on printing of graphene are actually based on graphene oxide (GO) that requires post-printing reduction to regain the electrical properties of pristine graphene.[22,44–50] Therefore, successive utilization of graphene for printed electronics requires ink formulations with high graphene loading, which should be stable against aggregation.

Preparation methods for metal, graphene, and CNT-based inkjet inks, which are suitable for printed electronics, and post-printing processing methods for obtaining high electrical conductivities, will be described in the following sections, addressing the above challenges.

3. Metal Nanoparticles

An important stage in the optimal formulation of metal-based conductive inks is the synthesis of metal NPs, which is required to fit the requests for specific performance of the devices to be printed. Especially important characteristics of the fabricated NPs are their average size and distribution, the shape of the particles, and the type of protecting agents on the particle's surface. Tuning these characteristics is achieved by correct selection of the reaction conditions (temperature, pH, sequence and rate of the reagent addition, etc.) and proper selection of functional additives. Sometimes, specific tailoring of the NPs surface is essential in order to match the requirements and performance of non-traditional sintering processes, for example adapting the inter-particle interactions to room temperature chemical sintering (see section "Post-Printing Treatment and Resistivity").

3.1. Synthesis of Metal NPs

Two main approaches are used for the preparation of metal NPs: top-down and bottom-up.

By the top-down approach, the particles are formed by breaking bulk metal into small particles and dispersing them in a proper medium. These methods include mechanical grinding, laser ablation in a proper liquid, rapid condensation of metal vapor obtained by electro-explosion of a metal wire, thermal heating, or plasma excitation of metal plates, powders or wires followed by its transport with a stream of an

inert gas (N_2, Ar) onto a solid substrate or into a liquid.[51–55] The main disadvantages of these top-down methods are the difficulties in obtaining large quantities of uniform NPs and the high cost due to high energy-consumption, as well as the need for sophisticated equipment.

By the bottom-up approach, NPs are formed from ionic precursors by reaction with a proper reducing agent in solution, or by the decomposition of precursor molecules.[15,55–60] Preparation of metal NPs by the "wet chemistry" processes is usually performed in an aqueous medium or in organic solvents.[15,56,57,59] Formation of metallic NPs in solution yields a great variety of dispersions with various particle characteristics such as size distribution, morphology and stability. The control of these properties can be achieved by varying the experimental parameters of synthesis such as concentration of reagents, redox potentials of the reducing agent, temperature, pH, rate of reagent addition, addition of pre-formed seeds, type and concentration of protective agents, etc.[15,61–65]

Since the first step in forming metal NPs in liquid is the reduction of metal ions to metal atoms, the driving force of the reaction is the difference in the reduction potential of the metal and the reducer, ΔE^0, which is related to the free energy of the redox process:

$$M^{n+} + Red = M^0 + Red^{n+} \quad \Delta G^0 = -nF\Delta E^0 \qquad (1)$$

As follows from the above equation, reduction is possible only if ΔE^0 is positive. This means that the reduction potential of the reducing agent should be more negative than the reduction potential of the metal precursor. Practically, the difference should be larger than 0.3–0.4 V; otherwise the reaction may proceed too slowly to be of practical importance.[63]

For the synthesis of metal NPs in aqueous medium, cations of strongly electropositive metals, such as Ag^+ (ΔE^0 = 0.8 V), Au^{3+} (ΔE^0 = 1.5 V), Pt^{2+} (ΔE^0 = 1.2 V), and Pd^{2+} (ΔE^0 = 0.99 V) can be reduced by relatively mild reducing agents; cations of moderately electropositive metals, for example, Cu^{2+} (ΔE^0 = 0.34 V) require stronger reducing agents, while cations of electronegative metals, such as iron (ΔE^0 = –0.04 V for Fe^{3+} and –0.44 V for Fe^{2+}) and Ni^{2+} (ΔE^0 = –0.8 V), can be reduced only by strong reducing agents, and the reaction proceeds usually at elevated temperatures.[15,66]

Many various inorganic and organic reducing agents have been applied to synthesis of metallic nanoparticles. The most often used are borohydride, BH_4^- and hydrazine, N_2H_4, which are strong reducing agents, more effective in alkaline medium (ΔE^0 = –1.24 V and –1.16 V, respectively)[57], citrate (ΔE^0 = –0.56 V), and ascorbic acid.[1] The latter is a weak reducing agent and, therefore, is effective only in reactions with ions of strongly electropositive metals. Ions of strongly electropositive metals can also be reduced by organic compounds containing oxidizable hydroxyl and carbonyl groups, such as alcohols with α-hydrogen, aldehydes, carbohydrates, and others.[15] Sodium phosphinate was also used as a reducing agent for the synthesis of copper NPs.[33,67]

Among organic solvents which were used for synthesis of metal NPs, the most reported are polyols (ethylene glycol, propylene glycol, diethylene glycol), which can act both as solvents for the metal precursor and as reducing agents. The reactions can be carried out at rather high temperatures, up to 250 °C, and finely dispersed NPs are usually produced. Since polyols are mild reducing agents, they are more suitable for obtaining NPs of electropositive metals, such as silver, gold, palladium, and platinum.[56,68,70] The polyol method is also widely used for the mass fabrication of silver nanowires.[69,71,72]

Among other organic solvents, toluene is also often used as a reaction medium for the reduction of metal NPs precursors.[73]

Metal NPs can also be produced by electrolysis of a metal salt in solution,[74–76] as well as by sonochemical[77,78] and sonoelectrochemical[79,80] methods. High energy radiation (UV-, γ-, and electron beam) were also applied in order to obtain dispersions of metal NPs.[81–83]

It should be emphasized that although there is a very large number of publications regarding wet synthesis of metallic NPs, the majority of these reports describes processes that are conducted at very low metal concentration. Obviously, in order to prepare inks with industrial importance, the dispersion of NPs should be at a high metal load, either requiring synthesis at high metal precursors concentration (which is problematic, as will be described later), or by concentrating the initial dispersion, a step which involves additional production costs.

3.2. Stabilization of Metal NPs

3.2.1. Stabilization of Dispersions

The fundamentals of stabilization are common to all types of NPs, whether inorganic or organic. Brownian motion of NPs in colloidal dispersions results in their collision and aggregation followed by coagulation and sedimentation, since the density of metal is much higher compared to the density of typical liquids. To be of practical importance to inkjet inks, the metal NPs should possess high colloidal stability. The best approach to preventing the aggregation of NPs is to stabilize them at the early stages of their formation by adding a proper dispersing agent during synthesis. Selecting the proper stabilizer and composition of the liquid vehicle is of great importance, since these components affect the shelf life and performance of the ink. Since the stability of nanomaterials is governed by the balance of various interactions, such as van der Waals attraction and electrostatic and steric repulsion, the optimal approach to obtain stable dispersions would be by using dispersing agents which have good affinity to the surface of the metal NPs and provide electrostatic, steric or electrosteric stabilization.

Electrostatic stabilization mechanism is based on electrostatic repulsion between electrical double layers surrounding interacting particles. The crucial condition for obtaining stable dispersions is the value of the surface potential of the NPs: the higher it is the larger the electrostatic repulsion and the more stable the colloidal system. As an indication of the surface potential, the zeta potential (ζ) of the particles is usually used. Dispersions of colloidal particles in water are considered stable at $|\zeta| > 35$–40 mV (at 1:1 electrolyte concentration of $<10^{-2}$ mol dm^{-3}).[15] Since the thickness of the

electrical double layer decreases with the increase in ionic strength, the particles can approach each other closely, collide and flocculate. Having in mind the need for high metal load dispersion for conductive inks, it is clear that this can be achieved while using high concentration of metal ions. However, this would lead to increased ionic strength and, therefore, unstable dispersion and aggregation already at the synthesis step.

To overcome this problem and in view that the electrostatic mechanism is not effective in organic media with low dielectric constant, steric stabilization mechanism is frequently utilized. Steric stabilization is achieved by surrounding the particles with the adsorbed layer of bulky molecules, such as molecules of a surfactant or a polymer, mostly of a nonionic type (detailed explanation of this mechanism is beyond the scope of this review). In principle, these molecules create a barrier which prevents close contact of particles and their aggregation. Steric stabilization is especially useful for concentrated dispersions of metal NPs. Nonionic amphiphilic polymers, which contain both hydrophobic and hydrophilic components and are capable of interacting with both metal NPs and a dispersion medium, are the most effective steric stabilizers. Among them, poly(*N*-vinyl-2-pyrrolidone) (PVP) is the most frequently used for stabilizing metal NPs in various liquids and in Ag- and Cu-based ink formulations.[15,33,62,69,76,80,84–100] This polymer strongly interacts with metal NPs through the oxygen atom of the carbonyl group.[101]

In the case of charged polyelectrolytes, both electrostatic and steric mechanisms are simultaneously involved, resulting in electrosteric stabilization of the colloidal particles. The electrosteric mechanism is especially effective in aqueous dispersions. Examples of such stabilizers for metal NPs and inks are: poly(acrylic acid) salts,[29,102,103] carboxymethyl cellulose sodium salt,[81,104] poly(diallyldimethylammonium chloride),[105] poly(ethyleneimine),[106] commercial dispersants such as polynaphthalene sulfonate (Daxad 19 of Hampshire Chemical Corporation,[64] high molecular weight block copolymer with acidic affinic groups (Disperbyk-190 of BYK-Chemie,[16] anionic phosphated alkoxylated polymer (Solsperse 40,000 of Lubrizol Advanced Materials), [107] and poly(carboxylate ethers) (Sokalan HP80 of BASF).[107]

3.2.2. Stabilization against Oxidation

At present, most conductive inks are based on silver NPs, since of all metals, silver possesses the highest electrical conductivity and is resistant to oxidation. Such inks are already commercially available (at least 10 companies in the United States, Japan, Korea and Israel produce Ag-based conductive inks). A very promising material for printed electronics, which can replace silver, is copper. Its conductivity is only 6 percent lower than that of silver, while its cost is less than a few % of the price of silver. However, spontaneous formation of copper oxides (both, Cu_2O and CuO) on the surface of the NPs at ambient conditions has two negative consequences: substantial decrease in electrical conductivity and an increase in the sintering temperature. Due to the significant cost reduction expected from using copper inks, the synthesis of air-stable copper NPs and Cu-based inks have attracted great interest in recent years.[26] The general approach to overcoming the oxidation issue is by performing the synthesis in organic solvents (polyols,[1,32,33,68,98,108,109] octyl ether,[110] octylamine,[111] toluene,[73] heptanes,[112]) often under inert atmosphere (Ar, N_2),[73,110–112] as well as minimizing the exposure of copper NPs to oxygen by forming a protective layer that surrounds the NPs ("capping agent"). Such protective layers are composed of carboxylic acids (lauric, oleic),[31,73,110,111] C_6-C_{18}-alkanethiols,[31,113] surfactants such as anionic bis(ethylhexyl)hydrogen phosphate (HDEHP),[112] cationic cetyltrimethylammonium bromide, (CTAB),[68] and polymers.[26] Polymers are the most effective of the above stabilizers, since the polymeric layer is dense enough to effectively slow down the oxygen penetration to the NP surface and, accordingly, the oxidation rate. The most widely used, both in organic solvents and in aqueous medium, is PVP which forms a densely packed, adsorbed layer on the surface of the copper NPs.[26,32–35,114] Long-term stability of copper NPs to oxidation was achieved by performing synthesis in water in the presence of CTAB[115] and CTAB-PVP mixture.[116] Stable copper NPs were also obtained by the formation of a copper formate shell, which was induced by a reaction of an interfacial copper oxide with formic acid. Such shell can be transformed into copper at a low temperature, resulting in highly conductive metallic films.[117]

One more approach to stabilizing copper NPs against oxidation is the use of antioxidants. It has been reported that ascorbic acid, which is a good scavenger of free radicals and reactive oxygen molecules, significantly retards the rate of Cu NPs oxidation.[118]

Nevertheless, all above methods do not prevent, but only retard oxidation, and are not yet applicable for fabrication of copper NPs with long-term stability. An effective approach to obtaining stable metal NPs, which can be further used as precursors for conductive inks, is the formation of a dense shell composed of non-oxidizable conductive material. For example, 50 nm copper NPs, coated with a ~3 nm layer of graphene by the reducing flame technique, were shown to be stable to oxidation at temperatures up to 165 °C. The disadvantage of such NPs is the low conductivity of the obtained coatings, five orders of magnitude lower than that of bulk copper.[119]

To overcome the oxidation issue and to obtain highly conductive coatings, an effective approach is the formation of bimetallic core-shell (core@shell) NPs with a protective shell made of noble metals (Au, Ag, Pt, Pd). There are several methods for the preparation of core@shell NPs,[120] but only two are suitable for obtaining dispersions of such NPs without noticeable admixture of mono-metallic NPs. One of the methods is based on the use of a reducing agent, immobilized on the surface of core pre-particles.[121] The second method is based on transmetallation reaction, which is a galvanic displacement reaction, when the surface of a preformed core is sacrificed as a reducing agent for the second metal with higher reduction potential. The result of such reaction is the formation of a second metal shell on the top of the core metal. Compared to other methods, transmetallation has two main advantages: first, no additional reducing agent is required, and second, reduction of secondary metal

occurs only on the surface of core, thus avoiding self-nucleation of the shell metal in solution. One more advantage is the possibility of preparing the core@shell NPs while retaining the original morphology of the core materials, such as plates, cubes, rods, and wires. The transmetallation method was used for synthesis of Co@Au, Co@Pd, Co@Pt, Co@Cu,[122] Ni@Au,[123] and Cu@Ag[23,29,124] NPs. It has been demonstrated that copper NPs, coated by silver shell, possess high stability in air at temperatures of up to 150 ºC.[29,125] Retaining their initial characteristics for at least two years makes them good nanomaterials for conductive ink formulations for printed electronics.[23,29]

4. Graphene and Carbon Nanotubes: Properties and Synthesis

4.1. Graphene

Two-dimensional single-layer graphene flake has a thickness of 0.34 nm corresponding to interlayer spacing of graphite.[22,24,45,126] Graphene sheet is characterized by a very high Fermi velocity (106 m s^{-1}) and a high intrinsic in-plane conductivity.[24,127] As has been predicted, the sheet resistance of graphene varies with a number of layers, N, as $R_s \sim 62.4/N\ \Omega/\square$ for highly doped graphene.[128]

Graphene and its derivatives are produced by several methods: from graphite by mechanical[129] and liquid phase[42,130–133] exfoliation, chemical vapor deposition (CVD),[134–136] solvothermal synthesis from organic compounds,[137] by chemical cross-linking of polycyclic aromatic hydrocarbons,[138] and by thermal decomposition of SiC.[139,140] However, compared to pristine graphene (PG), graphene oxide (GO) is more often used as a prercursor for formulation of conductive inks because of its dispersability in water and high electrical conductivity after post-printing reduction, which can be performed by chemical or thermal treatment.[6,141,142] GO is usually obtained by oxidation of graphite powder in the presence of strong acids and oxidants.[6,45,48,141–144]

4.2. CNTs

CNTs are cylindrical hollow nanostructures with walls composed of one-atom-thick sheets of carbon with graphene structure. Depending on the chirality along the graphene sheet, CNTs possess semiconducting or metallic properties. They exist both as single-walled (SWCNTs) and as multi-walled (MWCNTs), and their length is from less than a micron up to tens of microns (note: in this review we will not discuss graphene although it is an excellent conducting material, since it is less mature than CNTs in the field of printed electronics).

The diameter of SWCNTs is typically in the range of 0.4–4 nm, while the outer diameter of MWCNTs is in the range of few to tens of nanometers.[6]

The intrinsic electrical resistivity of individual CNTs was found to be as low as $10^{-6}\ \Omega\cdot$cm for SWCNT[24,145] and $3\cdot10^{-5}\ \Omega\cdot$cm for MWCNT.[146] However, in most cases, due to the presence of various defects or impurities formed during the CNT synthesis, the resistivities of individual CNTs, as well as the resistivities of their assemblies, were much higher.[147] Introducing acceptor dopants into CNT conjugated systems by oxidation in air or HNO_3, resulted in increased conductivity of CNT fibers.[147]

Because of the superior mechanical properties of individual CNTs, thin films made of randomly distributed CNTs were shown to possess unique mechanical properties such as flexibility and stretchability, which are essentially important for the fabrication of flexible electronic devices.

CNTs are produced by three major methods: electric arc discharge (a high temperature method – above 1700 ºC), laser ablation, and chemical vapor deposition (CVD).[8,36,148–150] The most often used is the DC discharge between two graphite water-cooled electrodes with diameters of 6–12 mm, in a chamber filled with helium at sub-atmospheric pressure, although hydrogen and methane gases are also used.[150] Usually, MWCNTs are produced by this method, if no catalyst is used. SWCNTs are usually produced when a transition metal catalyst (Fe, Ni, Co, Mo, Y) is used.[150] Laser evaporation/ablation (Nd:YAG or CO_2 lasers) of pure graphite targets is one of the superior methods to grow high quality and high purity SWCNTs.[150] Catalytic CVD, thermal or plasma enhanced, which is the catalytic decomposition of hydrocarbons or carbon monoxide, is now the standard method for production of high purity CNTs. The most frequently used catalysts are Fe, Co, or Ni.[149,150] CNTs were also fabricated by flame pyrolysis, using carbon monoxide as a carbon source.[151] Bottom-up organic synthesis of homogeneous CNTs with a well-defined structure was recently demonstrated.[152] The method is based on utilizing hoop-shaped carbon macrocycles, which are used as templates for polymerization reactions to produce long CNTs. MWCNTs were also produced by hydrothermal processing of a mixture of polyethylene and water, or ethylene glycol and water, with a Ni catalyst at 700–800 °C under pressure of 60–100 MPa,[153,154] and by the electrolytic process, which involves graphite cathode immersed in molten chlorides of alkali, or alkaline-earth metals.[148,149]

5. Formulation of Conductive Inks

Inkjet ink for printed electronics contains a conductive nanomaterial, aqueous or organic liquid vehicle, and various additives that enable optimal performance.[1,6,12,16] Since inks should provide high electrical conductivity of the printed patterns, it is essential that the content of the conductive nanomaterial be high: the higher its concentration in the ink, the better conductivity at a given droplets size. The latter depends also on the presence of non-conducting materials between the particles, such as organic polymeric stabilizers, wetting agents and adhesion promoters. Therefore, a prerequisite for obtaining a conductive printed layer is forming direct electrical contacts between the conducting nanomaterials in the printed pattern. In case of metallic NPs, this is achieved by performing a sintering process, for example by heating and decomposing the organic insulating materials.[1]

NANO MICRO small

5.1. Metal-Based Inks

To be of practical importance, conductive metal-based inkjet inks should have high metal loading in the range of 20–80 wt%.[2] Although, the final conductivity of printed patterns depends on several factors, including sintering methods (see next section) and the number of printed layers, high metal loading in ink formulation usually provides higher conductivity at one-layer printing, since the more concentrated the dispersion of metal NPs, the higher number of contact points and percolation paths between NPs in the printed layers.

There are only a few reports on direct preparation of concentrated dispersions of metal NPs,[1,155] and, therefore, most methods of formulating inks with high metal loading are based on the two-steps procedure. During the first step, the synthesized NPs are separated by centrifugation, or by precipitation with alcohols (such as methanol, ethanol, isopropanol) or acetone, followed by washing of the sediment with a proper solvent to remove excess dispersion stabilizers. In the second stage, the obtained NPs are dispersed in a proper liquid vehicle containing the required additives. This approach was successfully used for preparing Ag-based,[16,91,95,100,156–160] Cu-based,[32,33,73,96,111] and Cu@Ag-based[161] inks. Metal nanopowders prepared by the gas-phase,[52] laser ablation,[120,162,163] and mechanochemical[164,165] methods can also be used for conductive ink formulation. Typical solvents for metal-based inks are water,[16,26,100,157,166] hydrocarbons,[158,160,167–170] alcohols and other oxygenated solvent.[33,84,168,171–173] However, to tailor inkjet inks for optimal printing performance, the ink vehicles should usually be composed of a mixture of solvents, such as water with alcohols[85,86,89] and glycols,[76,82,98] as well as multicomponent mixtures containing water, organic solvents and glycerol.[85,86,95,107] Commercially available Ag-based conductive inks with NPs size in the range of 2–200 nm and metal loading in the range of 10–60 wt% are now being produced by Cabot (USA), NovaCentrix (USA), Sun Chemicals (USA), NanoMas (USA), Applied Nanotech (USA), InkTec (Korea), Harima Chemicals (Japan), Advanced Nano Products (Korea), Samsung Electro-Mechanics (Korea), Cima NanoTech, PV Nano Cell and XJet Solar (Israel). A number of nanoparticulate Cu-based conductive inks containing 10–40 wt% metal (particles size 25–130 nm) are also produced by NovaCentrix (USA), Intrinsiq Materials (USA), Applied Nanotech (USA), and Samsung Electro-Mechanics (Korea).

5.2. Graphene-Based Inks

Dispersions of PG are usually prepared by ultrasonication of graphite in water or organic solvents such as terpineol,[44] N-methylpyrrolidone, γ-butyrolactone, 1,3-dimethyl-2-imidazolidinone,[22,130,133] *o*-dichlorobenzene,[133] and ethanol.[174] To obtain stable dispersions suitable for inkjet ink formulations, various stabilizing agents are used: polycyclic aromatic hydrocarbons;[43] surfactants such as sodium dodecyl sulfate (SDS),[50] sodium dodecylbenzene sulfonate (NaDDBS),[131] sodium deoxycholate,[133] sodium cholate,[175,176] and CTAB;[177] polymers such as PVP[178] and PVA;[179] and ethyl cellulose.[44,174] One of the major disadvantages of such dispersions is the low graphene loading, which is usually in the range of 0.002–0.1 wt%.[22,43,133,178]

GO contains hydroxyl, epoxy, carbonyl and carboxylic groups that makes it easily dispersible in water[22,45,48,180] and polar organic solvents such as *N,N*-dimethylformamide (DMF), *N*-methyl-2-pyrrolidone (NMP), tetrahydrofuran (THF), and ethylene glycol.[181] Preparation of stable GO dispersions does not require addition of stabilizing agents that is obvious advantage of GO-based inks compared to PG-inks. The concentrations of GO in inks is usually in the range of 0.1–1.0 wt%.[45,47,49,141]

5.3. CNT-Based Inks

As had already been mentioned, the major challenge in formulating CNT inks is to obtain a stable dispersion of non-aggregated nanotubes in a proper liquid vehicle, at low viscosity. Since the CNTs are very hydrophobic, three routes for obtaining such dispersions are presented: (a) dispersing the CNTs in organic solvents without dispersing agents,[21,24,36,182–184] (b) dispersing the CNTs in an aqueous media using dispersants such as surfactants (anionic, cationic, and nonionic) or polymers,[23,24,36,41,185–190] and (c) chemical modification of the CNT with functional groups, which favor the interactions of CNTs with the dispersing medium[24,36] (for example, to obtain water-dispersible CNTs, nitric acid is usually used to produce oxygen-containing carboxyl, carbonyl, and hydroxyl groups on the surface of a nanotube).[191,192] The major problem with organic solvents without dispersing agents is the inability to obtain dispersions with high CNTs concentration, more than 0.1 g L^{-1}.[24] To obtain aqueous dispersions of CNTs, the surfactants Triton X-100[41,187,193,194] and SDS[187,190,193,195,196] are the most widely used. Other reported surfactants are Tween 20 and Tween 80,[187] sodium cholate,[189] CTAB,[197] dodecyl trimethylammonium bromide (DTAB),[195] and NaDDBS.[193] Stabilization is achieved due to adsorption of the hydrophobic tails of the surfactant molecules on the nanotube surface, while the hydrophilic head groups are directed toward the aqueous phase. Polymeric stabilizers are rarely used.[23,186] For all solubilization schemes, the energy must be applied to the system in order to break the CNT aggregates. The most widely used approach to prepare homogeneous dispersions of CNTs is ultrasonication for a prolonged time.[23,182–185,188–192] An alternative method for de-agglomerating CNT bundles is based on high pressure homogenization.[41,198] It was also reported that superacids enable dispersion of the CNTs without applying high shear forces. For example, chlorosulfonic acid was identified as a true solvent for CNTs because it protonates the side-walls, dissolves the CNTs as individuals, and promotes the formation of liquid crystals from a wide range of nanotube sources, including multi-walled nanotubes and long carpet-grown CNTs.[199]

CNT inks for conductive printing can be formulated by combining the above dispersions with suitable additives, according to the required printing method, and in order to improve printing performance. Liquid vehicles are

water,[23,185,189–191] organic solvents such as DMF,[21,182,183] *N*-methyl-2-pyrrolidone,[184] and γ-butyrolactone,[188] as well as solvent mixtures.[10,200,201] Typically, the content of CNTs in ink formulations is in a wide range of concentrations, 0.01–10 g L^{-1}.[10,21,23,182,185,190,191,200,202] It should be noted that in many reports the actual concentration of CNT is not known, since the dispersion is either filtered or let to sediment prior to printing in order to separate the large CNT bundles. Concentration limitation is important in the printing methods, which require low viscosity ink (such as inkjet or flexo), but less crucial, for example, in screen printing. Recently we reported on a inkjet ink with good printing performance at 10 g L^{-1} MWCNTs, dispersed in water with the use of 0.5 wt% polymeric dispersant (SOLSPERSE 46000 of Lubrizol, USA), and 0.1 wt% of wetting agent (Byk 348 of Byk-Chemie GmbH, Germany).[23] A number of printable nanocomposite inks, containing CNTs and silver NPs[203,204] and CNTs and PEDOT-PSS[205,206] were also reported. As for commercial CNT-based inks, to the best of our knowledge, there is a very small number of products in the market, such as Nink-100 (MWCNT ink) and Nink-1100 (SWCNT ink) of NanoLab Inc. (USA). These inks contain carboxyl (COOH) functionalized carbon nanotubes in an aqueous suspension, with the minimum concentration of additives to impart long-term stability and printability to the ink.

5.4. Inks for Printing Conductive 3D Structures

Additive manufacturing by printing has become an attractive field of research and industrial activities. So far, most efforts have been devoted to materials design and printing approaches for the production of 3D structures, but it is clear that there is a future need for functional 3D structures, including conductive ones. Inkjet printing is a major 3D printing technology, and its main challenge is to enable rapid fixation of the printed pattern on a substrate, in spite of the low viscosity of the ink. Two main types of conductive inkjet inks for printing 3D structures have been studied: metal NPs dispersed in volatile solvents, and metal NPs dispersed in UV-curable liquids. When using the first approach, metal pillar arrays, helices, zigzags, and micro-bridges are built on heated substrates by printing dispersions of gold NPs in toluene or α-terpineol.[207,208] Upon contact of the ink droplets with the heated substrate, the solvent immediately evaporates, thus increasing significantly the metal load and the viscosity, and enabling fixation of each drop (with obvious shrinkage in droplet volume). UV-curable inks contain monomers or oligomers (such as acrylate derivatives) and photoinitiators capable of rapid polymerization upon irradiation with UV light, thus enabling immediate fixation of each droplet, leading to a 3D structure by layer-by-layer printing on the same spot.[12,209]

Combining UV-curable composition with conductive NPs enables fabrication of conductive 3D patterns.[210,211] For example, resistors were printed by using UV-curable inks based on a poly(ethylene glycol) diacrylate (PEGDA) matrix and containing a dispersion of aqueous silver NPs (10 to 50 wt%). For resistors, the presence of a large amount of insulating material, such as polymerized monomers, is not very crucial. However, to obtain high conductivity, these materials present an obstacle. To overcome this and to enable suitable percolation paths of the metallic NPs, we prepared a new, two-phase ink, in which one phase brings conductivity and the other, 3D structuring. This ink is composed of oil-in-water emulsion, in which the oil phase contains polymerizable acrylate monomers with a mixture of initiators, and the water phase contains 30 wt% dispersion of silver NPs. The ink was successfully applied in layer-by-layer printing of 3D conductors, and conductivity was achieved after a post-treatment based on chemical sintering, as will be discussed later. A scheme of the printing process is shown in **Figure 1**.[211]

6. Post-Printing Treatment and Resistivity

6.1. Electrical Resistivity

Electrical resistivity is an inherent property of bulk materials, and is defined as follows:

$$\rho = R \cdot A / L \tag{2}$$

where ρ is the resistivity (Ω·m, or μΩ·cm), R is the measured resistance of a conductor, A is its cross-sectional area (A = h·W, where h is film thickness and W is its width), and L is film length.[2]

In practice, for films in printed electronics, the most commonly used value is the sheet resistance, which is defined as follows:

$$R_{sq}\,(or\,R) = \rho / h \tag{3}$$

Sheet resistance (Ω/□) can be directly measured by a four-point probe and is convenient for comparison of the resistivity of various printed patterns, without the need to measure the film thickness.

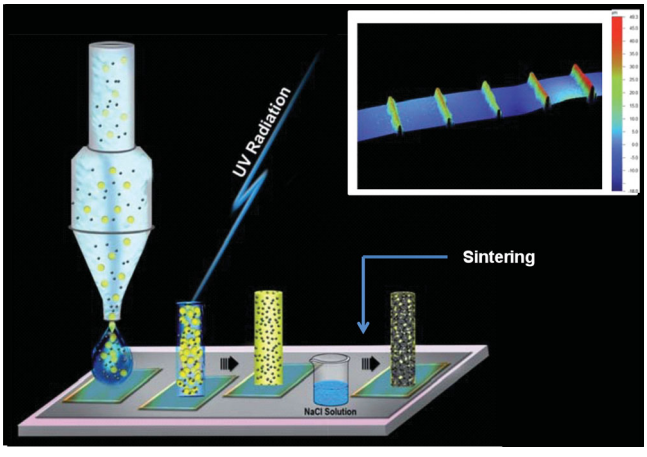

Figure 1. Printing of a conductive 3D structure with the use of ink composed of an UV-curable emulsion and a dispersion of metal NPs. Inset is a 3D profile of a 200 μm width lines composed of 1, 3, 6, 10, and 20 printed layers. Reproduced with permission.[211] Copyright 2013, The Royal Society of Chemistry.

small NANO MICRO

6.2. Sintering and Resistivity of Printed Metallic Patterns

Application of conductive nanomaterials for printed electronics should address two main challenges: first, the need to obtain high electrical conductivity of the printed pattern, desirably close to that of bulk metal, and second, the need to achieve high electrical conductivity under relatively mild conditions, at which the properties of the substrate material are not affected (this is especially important for plastic electronics).

In the case of metallic NPs, after drying the ink, the presence of remaining organic stabilizing agents and other non-volatile components of the ink in between the particles, prevents the close contact of particles, thus preventing the formation of continuous metallic contact that results in low electrical conductivity. Therefore, a post-printing process in which the particles are sintered, is required. Sintering is a process of welding particles together without their melting,[2] and usually requires the removal of organic materials (for example, by decomposition). This can be easily achieved by thermal decomposition of the organic materials at elevated temperatures, in the case of substrates such as glass and silicon. This process it routinely used for sintering the conductive patterns on silicon solar cells. Nowadays, there is great interest in flexible electronics,[1,17] in which the substrates are made of polymers which are usually heat sensitive, e.g. polyethylene terephthalate (PET) and polycarbonate (PC). Therefore, the current development of various sintering methods focuses mainly on avoiding destruction of the polymeric substrates. This can be achieved by exposure of the printed pattern to heat (thermal sintering at low temperature), intense light pulse (photonic sintering), microwave radiation (microwave sintering), plasma (plasma sintering), by applying an electrical voltage (electrical sintering), and by contact with chemical sintering agents at room temperature (RT sintering). In addition, printed patterns should retain high adhesion to the substrate after post-printing treatment since some of sintering methods (e.g. photonic sintering) are "top-downwards" methods (metallic layer forms from the top of printed feature down to the substrate).

6.2.1. Thermal Sintering

Heating is the conventional method for metal NPs sintering. Because of the high surface-to-volume ratio and enhanced self-diffusion of the metal atoms, metal NPs are characterized by decreased melting point as compared to bulk metal. For example, for silver and gold particles with a diameter of 2.5 nm, a reduction in melting point was estimated to be around 400 and 500°C, respectively.[212,213] The melting point of 1.5 nm gold particles was experimentally found to be 380 °C (compared to the melting point of bulk gold, 1063 °C).[213] Even for 20 nm particles, the melting point was found to be noticeably lower than that of the bulk metal.[213] Enhanced self-diffusion of surface atoms induces initial neck formations between adjacent NPs in the printed patterns, followed by formation of numerous percolation paths at temperatures much lower than the melting point. Usually, heating at 200–350 °C for 10–60 min is required to remove the organic

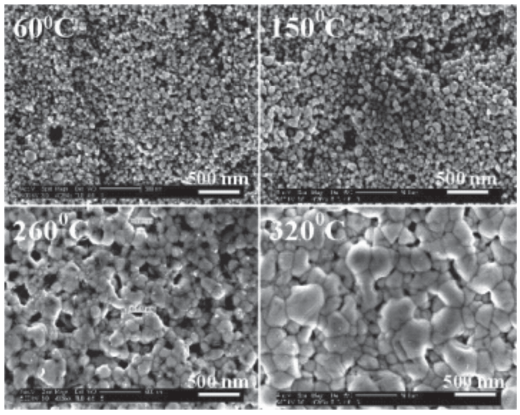

Figure 2. SEM images obtained with silver ink deposited on a glass slide and heated at various temperatures. Reproduced with permission.[16] Copyright 2005, Wiley-VCH Verlag GmbH & Co. KGaA.

insulating materials from the surface of the NPs, and to obtain sintered metal coatings with resistivity comparable to that of bulk metal, for both, silver-based[1,73,84–86,91,95,120,160,169,214–216] and copper-based[33,73,76,88,96,109,217,218] inks. **Figure 2** shows the typical changes in morphology of a silver printed layer after heating at various temperatures for 10 min. The critical changes in morphology with the formation of a continuous interconnection between silver NPs are clearly seen at 260 °C. At 320 °C the layer is well sintered (yielding half the conductivity of bulk silver).[16]

There are several reports on metal inks with sintering temperature of <200°C. Lowering the curing temperature has been achieved by properly tailoring the composition of the ink, mainly by using short stabilizers or ones that decompose at low a temperature. For example, ink with gold NPs stabilized by alkanethiols with 4–6 carbons, can be sintered at <150°C with resulting conductivity of 70% of bulk gold.[219] Ink formulation containing low concentrations of weakly adsorbing stabilizers, like poly(ethylene oxide) and poly(vinyl alcohol), enables to obtain conductive silver lines (5% of bulk silver conductivity) after sintering at 80 ºC for 60 min.[220]

As to adhesion issue, the adhesion strength depends both on the substrate material and the sintering temperature. It has been demonstrated that adhesion of silver NPs to various polymeric substrates increases as the substrate hardness decreases. A drastic increase in adhesion was observed at temperatures slightly higher than the glass transition temperature (T_g), while further heating resulted in a decrease of adhesion.[221] In some cases strengthening the binding between thermally sintered printed metallic layer and substrate can be achieved by coating the last with a molecular adhesive layer, e.g. aminopropyltriethoxysilane[222] or by using metallic inks containing glass frit additives.[223]

6.2.2. Photonic Sintering

Photonic sintering utilizes flash lamps, lasers, and other light sources which deliver energy to the targeted material to be sintered.

For example, a photonic sintering technique, developed and commercialized by NovaCentrix (USA), generates

high-intensity millisecond light pulses and can be used for R2R processing. By careful control of the duty cycle of the lamps and the amount of delivered energy, the printed patterns can be effectively sintered without damage of heat-sensitive substrates. Photonic sintering starts at the surface layer of printed NPs. Heat transfer from the surface leads to sintering underlying NPs. This results in higher density of the surface layer compared to internal bulk.[224,225]

With this technique, sintered silver and copper printed layers with resistivities of 4 and 10 times of bulk metals, respectively, were obtained, while the morphology of the sintered layer was very similar to that at thermal sintering.[226] Sintering of copper inks printed onto polyimide (PI) with the use of a high-power pulsed Xe lamp resulted in resistivities 2.8, 4.6, and 11.6 times of bulk copper, depending on the ink vehicle (water/isopropanol, cyclohexanol/water/isopropanol, and isobutanol/water/isopropanol, respectively).[89] Similar results were obtained for ink composed of coppers NPs dispersed in a mixed solvent of ethylene glycol and 2-methoxyethanol.[227] Flash sintering of silver inks printed on PET resulted in resistivity only 4 times higher than the resistivity of bulk metal.[224,228] Sintering of silver inks printed onto paper with the use of IR lamp resulted in conductivity of about 10% of bulk metal.[229] Is has been shown that the adhesion of sintered films to plastic substrate improves with an increase in the number of flashes and energy input.[6,228,230]

Lasers, both continuous wave Ar ion[231–233] and pulsed Nd:YAG,[234] have also been utilized for sintering printed metallic patterns. Selective local laser sintering of inkjet printed metal NPs, followed by removal of ink which was not exposed to the radiation (unsintered particles), enables high-resolution patterning, thus overcoming the limitation of inkjet direct writing.[233] As has been demonstrated for gold ink, an increase in laser power resulted in strong film adhesion to silicon substrate.[235]

6.2.3. Plasma Sintering

Plasma sintering is usually performed by exposure of printed patterns to low pressure Ar plasma.[17,214,236] The sintering process shows a clear evolution starting from the top layer into the bulk. If the time of plasma action is not sufficient, the sintered top "skin" layer can be easily removed by applying adhesive tape.[17,237]

It has been shown that plasma at 80 W decomposes the organic moieties around the metal NPs, and after sufficient exposure time the NPs transform to bulk metal.[237] This method is applicable to plastic substrates, and the obtained resistivities of the printed patterns are ~10 times higher compared to the resistivity of bulk silver.[237] Recently, it was reported that low pressure Ar plasma post-treatment resulted in the conductivity of printed patterns equal to 11% of bulk silver after only 1 min of exposure, and 40% of bulk silver after 60 min of exposure, while the processing temperature was below 70 °C.[20] To avoid the need for sophisticated equipment for low pressure plasma sintering, Ar plasma sintering at atmospheric pressure and room temperature was developed. With this technique, 12% of bulk silver conductivity was reached within 4 seconds.[238] This approach enables sintering of patterns printed onto plastic substrates and can be utilized in R2R processes.

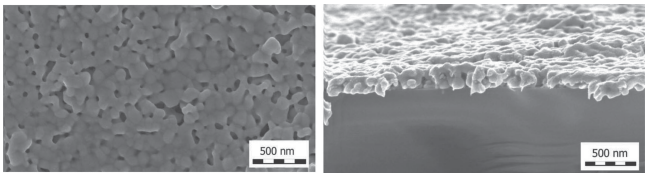

Figure 3. SEM micrographs of a sample obtained after sequential plasma and microwave sintering of printed silver track (left – top view, right – cross-sectional view). Reproduced with permission.[18] Copyright 2012, Wiley-VCH Verlag GmbH & Co. KGaA.

6.2.4. Microwave Sintering

Metals can be sintered quickly by microwave radiation, but they have a very small penetration depth, in the range of 1–2 μm for Ag, Au, and Cu at 2.54 GHz.[236,239] Therefore, microwave sintering can only be successful if the thickness of the printed object is in the range of the penetration depth. However, for metals such as silver, which is a good thermal conductor, the printed patterns will be heated uniformly by thermal conductance, enabling the microwave radiation to be applied to sintering patterns with a thickness exceeding the penetration depth. For example, treatment of silver patterns on PI with an average height of 4.1 μm, at constant-power (300 W) microwave reactor for 240 sec resulted in metallic tracks with conductivity 20 times lower than that of bulk silver.[239] Flash microwave sintering (1 sec) of silver tracks which were previously heated at 110 °C for 1–5 min, resulted in conductivity of 10–34% of bulk silver.[240] Combining photonic and microwave flash treatments enabled to obtain 40% of bulk silver conductivity in less than 15 seconds.[241] Even higher conductivity, 60% of bulk silver, was obtained in less than 10 min by combining low-pressure Ar plasma and microwave flash sintering of silver tracks printed on PEN foil, without damage of the polymeric substrate.[18] **Figure 3** shows the morphology of such track, which is very similar to the morphology obtained after thermal sintering (compare with Figure 2).

6.2.5. Electrical Sintering

By this method, sintering is reached by applying a voltage over the printed pattern that causes an electric current and leads to a local heating of the metallic layer. This method requires that the printed feature be slightly conductive before sintering.[17] The conductivity of silver track on photo paper obtained with the electrical sintering method, was reported to be more than 50% of bulk silver.[242] While the silver track temperature reached 130 °C, the substrate temperature stayed below 60°C.[243] The advantage of this method is the short sintering time (typically <100 msec,[243] although direct contact with a power supplier is necessary, and therefore this method cannot be applied to large area R2R printed electronics.[6]

6.2.6. RT Sintering by Chemical Agents

Several sintering methods, which can be performed even at room temperature, were recently developed (RT sintering). Most of them are based on coalescence of metal NPs triggered by chemical agents.

NANO MICRO small

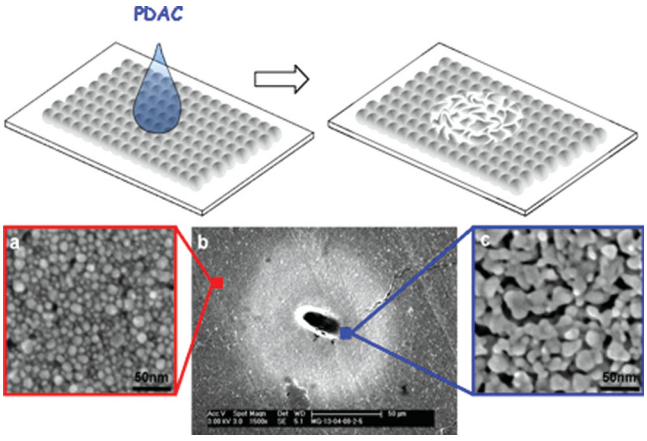

Figure 4. Schematic illustration showing what happens when a droplet of PDAC solution is printed on a silver NPs array, and SEM images of the printed silver nanoparticles (a,b,c). Images (a) and (c) show the magnified NPs arrays after contact with PDAC outside and inside the droplet zone, respectively. Reproduced with permission.[244] Copyright 2010, American Chemical Society.

It has been demonstrated that a polycation, poly(diallyldimethylammonium chloride) (PDAC) acted as effective coagulant for silver NPs, which were stabilized by a polyanion, poly(acrylic acid) sodium salt (PAA), and caused sintering of silver ink (30% Ag, average particle size 10 nm) deposited onto a solid substrate.[244] **Figure 4** shows that a drop of PDAC placed on a layer of silver NPs causes sintering of NPs without any heating. This sintering process also takes place when the silver ink is printed on a substrate which is pre-coated with PDAC solution. The resistivity of a silver pattern printed on photo paper pre-coated with the polycation was only 4.2 times higher than the resistivity of bulk silver.[244] A similar sintering performance was observed for Cu@Ag NPs (20–50 nm) printed on photo paper.[245]

Another concept for RT sintering of printed patterns is based on the removal of a stabilizing agent from the surface of NPs by chemical agents that enables coalescence of metal NPs. For example, in case of gold nanoparticles stabilized by 1-butanethiol, oxidation of the stabilizing agent by NO_2 resulted in the sintering of gold NPs followed by a noticeable decrease in resistivity.[246] It has also been demonstrated that contacting a silver printed pattern with NaCl solution followed by heating to 95°C, leads to noticeable decrease of resistivity.[247] A similar effect was observed after dipping the printed metallic lines (PVP-stabilized silver NPs) in saturated NaCl solution and ultrasonication. Such treatment caused the detachment of the PVP molecules from the surface of silver NPs, leading to their coalescence and sintering, and resulting in about 16% conductivity of the bulk silver.[248] The resistivity of the 3D pattern obtained by inkjet printing of UV-curable ink containing dispersed PAA-stabilized silver NPs (30 wt%) after dipping into 1 M NaCl solution (Figure 1), was found to be only 7 times higher than the bulk metal resistivity.[211] High conductivity, about 30% of bulk silver, was achieved by sequential printing of silver nanoparticles ink and a "sintering" ink composed of NaCl or $MgCl_2$ solutions.[249] Removal of the polymeric stabilizer in order to obtain high conductivity can also be accomplished by the exposure of printed patterns to HCl vapor.[250]

A new concept for conductive nanoinks based on a built-in sintering mechanism, which is triggered during the drying stage of the printed pattern, was recently developed. Silver nanoparticles that are stabilized by PAA undergo self-sintering spontaneously, due to the presence of a destabilizing agent, NaCl. Prior to printing, the concentration of NaCl is very low (up to 50 mM) and the ink is stable. After printing and during drying of the printed pattern, the concentration of the salt increases and it comes into action, causing a detachment of the polymeric stabilizer from the surface of NPs (**Figure 5**).[19] The obtained conductivity of the printed silver patterns was as high as 40% of bulk silver.

6.3. Resistivity of Graphene- and CNTs-Printed Patterns

6.3.1. Graphene

Because of low graphene concentration, to achieve low resistivity, multiple printing of graphene-based inks is usually required.[22,50] In addition, electrical resistivity can be significantly decreased by post-deposition annealing in air at 300–400 °C or at higher temperatures in inert atmosphere in order to remove the stabilizing organic material.[44,50] For example, 20 times lower resistance of inkjet printed patterns sintered at 400 °C for 3 h in Ar, was obtained for 200 printed layers as compared with 10 layers, and the resistivity of the graphene layer after 200 printings was found to be 16.68 Ω·cm.[50] Film composed of 5 PG layers printed onto glass slides and

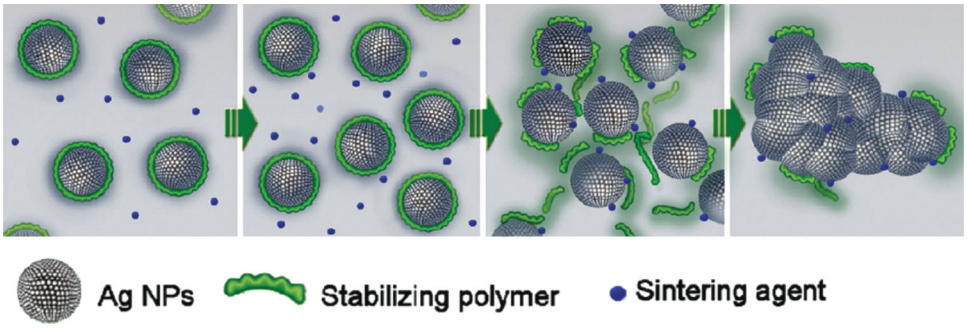

Figure 5. Schematic illustration of the stabilizer detachment and sintering of NPs caused by a built-in sintering agent. Reproduced with permission.[19] Copyright 2011, American Chemical Society.

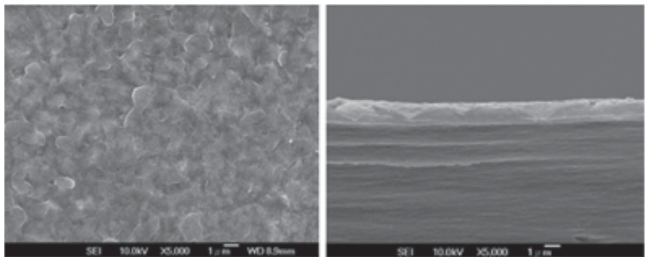

Figure 6. Field-emission SEM images of films obtained by printing 50 graphene layers onto polyimide substrate (left image – top view, right image – cross-sectional view). Reproduced with permission.[50] Copyright 2013, Elsevier.

annealed in air at 400 °C for 30 min had sheet resistance of 30 kΩ/□.[44] PG tracks printed on silica (10 printings, each printing adds ~14 nm to the line thickness) possessed resistivity of about $4{\cdot}10^{-3}$ Ω·cm after annealing at 250 °C for 30 min.[174] **Figure 6** shows the morphology of the film obtained by multiple printing the graphene layers onto PI substrate.[50]

To make the GO-printed films conductive, they should be reduced. Chemical (e.g. hydrazine vapor, hydrides) and thermal reduction (in inert atmosphere in the presence of a reducing gas, H_2), or combination of chemical reduction and heating are usually used.[6,46,141,144,148,180] Reduction of GO to graphene affects only the surface layer of deposited film, and the underlying material remains an insulator.[6] Thermal reduction is more effective than chemical reduction, but requires high temperatures (>550 °C) that is not suitable for heat-sensitive plastic substrates. Is has been demonstrated that treatment of GO films deposited onto SiO_2, Si, PET, ITO and metals with dimethylhydrazine vapor followed by annealing at 200 °C in N_2 resulted in sheet resistance of 43 kΩ/□.[180] Treatment of GO film inkjet printed onto PET substrate (30 printed layers) with hydrazine and ammonia vapors at 90 °C for 1 h resulted in sheet resistance of only 65 kΩ/□.[251] Resistivity of ~0.2 Ω·cm was reported for GO film inkjet printed onto PI and reduced by heating at 400 °C for 3 h in a mixture of Ar and H_2.[45] Even lower resistivity, ~0.01 Ω·cm, was obtained for GO film annealed in Ar/H_2 mixture at 500 °C for 2 h.[176] A new approach to obtaining conductive films of graphene (sheet resistance >100 kΩ/□) by reactive inkjet printing was recently reported. This approach is based on sequential printing of GO ink and ink containing a reducing agent, ascorbic acid mixed with $FeCl_2$, on a substrate heated to 60 °C.[252]

6.3.2. CNTs

Inks based on CNTs as the conductive material, usually do not require post-printing heat treatment.[191] The resistance of CNT-printed patterns is controlled by the ink composition, the number of printed layers and post-printing processes. Although the intrinsic electrical resistivity of individual CNTs is as low as 10^{-8} Ω·m,[24,145] the resistivities of CNT films are higher, and the reported values calculated from the experimental data are in a wide range – $7.8{\cdot}10^{-8}$ – $2.0{\cdot}10^{-3}$ Ω·m.[23,24,183,253–255] Usually, CNT films are characterized by sheet resistance, which is also in a wide range – 0.05–100 kΩ/□.[3,8,24,186,191,200,255–265] Higher resistivities of CNT films as compared with the intrinsic resistivity of individual CNTs are mainly related to the high resistance between overlapping CNTs in the random network (junction resistance), and to their electrical transport properties (e.g. relative content of metallic and semiconducting tubes).[8,261,266] Usually, longer CNTs lead to more conductive films, as this limits the number of CNT junctions per unit area.[24] Since for CNTs the hole mobility is larger than the electron mobility, the p-dopants, which are usually strong oxidizers such as concentrated HNO_3 (70%), NO_2, and $SOCl_2$, are effective agents for improving conductivity.[8] In addition, the contact resistance in the films is significantly improved by the removal or decomposition of residual solvents and dispersants by these agents.[254,260–262,267] For example, treatment of SWCNT films with HNO_3, $SOCl_2$ or their mixture resulted in 2–10 times decrease in sheet resistance.[253,254,257,259–265] The film resistance also decreases with the increase in the film thickness (number of coatings or printed layers).[185,191,202,263] **Figure 7** shows nanoscale morphologies of CNT conductive films. A film of SWCNTs on a glass slide formed by spin coating (Figure 7A) was characterized by sheet resistance of 59 Ω/□.[264] MWCNTs films, inkjet-printed onto a transparency film, had sheet resistance of ~30 MΩ/□ for 4 printed layers (Figure 7B),[202] and of ~20 kΩ/□ for 90 printed layers (Figure 7C).[191] Obviously, the latter two values are too low

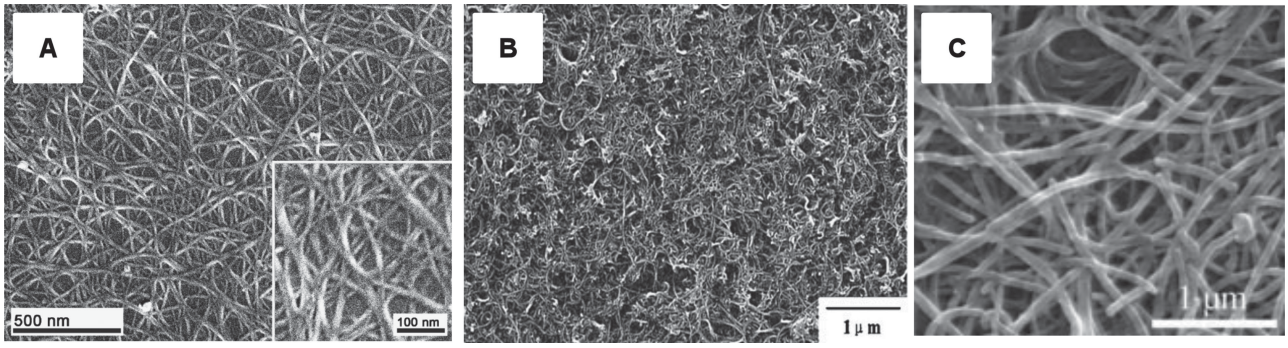

Figure 7. SEM images of CNT films. (A) SWCNTs film deposited onto a glass slide by spin coating.[264] Data reproduced by permission of the American Chemical Society. (B) 4 times inkjet-printed MWCNTs film on a transparency film.[202] Reproduced by permission of Elsevier. (C) 90 times inkjet-printed MWCNTs film. Reproduced with permission.[191] Copyright 2006, Wiley-VCH Verlag GmbH & Co. KGaA.

NANO MICRO small

for most applications and, therefore, SWCNTs are preferred for obtaining high conductivities.

7. Applications of Conductive Nanomaterials

In the following sections we will discuss several applications of conductive nanomaterials for the fabrication of printed electronic devices. This will include fabrication and properties of transparent conductive electrodes (TEs), which are nowadays essential features for many optoelectronic devices, and inkjet-printed devices, such as RFID tags, light emitting devices, thin film transistors and solar cells.

7.1. Transparent Electrodes

Over the last decade, the market for TEs has grown due to wide proliferation of LCD displays, touch screens, thin-film solar cells, and light emitting devices.[267,268] The dominating materials are sputtered metal oxides, but the most widely used is indium tin oxide (ITO) with a market share of more than 97% of transparent conducting coatings.[267] ITO coatings are characterized by low resistance, down to 10 Ω/□, at about 90% optical transparency in the visible range.[8] However, ITO coatings have several major drawbacks, such as high cost, expensive manufacturing and brittleness, the last one imposing severe limitation on its utilization in flexible electronics.[8,36,258,267] In addition, for various display applications, there is a need for patterning of the conductive material, which is made by chemical etching. Therefore, much effort is being made nowadays to find alternatives for ITO, which is based on nanomaterials, and which can be printed directly on various substrates without etching processes. An ideal replacement should be inexpensive, flexible, thin and simple in manufacturing films. Depending on the application, sheet resistance can be in the range of 10 to 10^3 Ω/□ at a transparency of ≥90%. 400–1000 Ω/□ is sufficient for many touch screen applications, and ~10–50 Ω/□ is required for OLEDS and solar cells.[24,260,269] In the next sections we will briefly present conductive TEs based on nanomaterials: nanosized metals (NPs and nanowires), graphene, and CNTs.

7.1.1. Metal Nanoparticles

A common approach to fabricating metallic TEs is by forming ultrathin (~10 nm) films deposited by DC sputtering, or by patterning grids by using imprinting lithography.[24,269–271] There are several methods for the fabrication of TEs, which are based on controlled wetting and self-assembly of metal NPs. Among them, Cima Nanotech developed a coating process that utilizes a silver dispersion with a volatile emulsion, which upon spreading and drying on a substrate, forms holes surrounded by thin silver lines (SANTE® Technology, Cima Nanotech). Another process is based on spontaneous self-assembly of NPs in metallic rings formed during evaporation of silver nanodispersion ("coffee stain" effect) with a conductivity of 15% of bulk silver.[272] To obtain transparent conductive coatings, a 2D array of overlapping metallic rings was formed by inkjet printing. The resulting array of silver rings with rims <10 μm in width and <300 nm in height (**Figure 8**) had a transparency of 95% and sheet resistance of 4 Ω/□.[273]

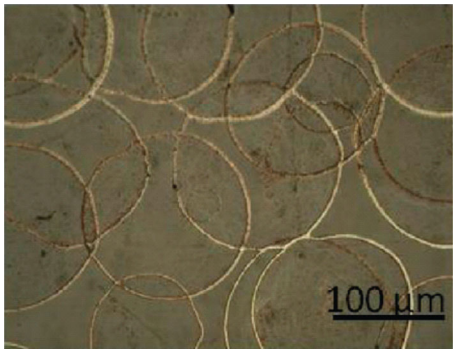

Figure 8. Array of interconnected rings formed by Ag NPs. Reproduced with permission.[273] Copyright 2009, American Chemical Society.

A third approach is based on patterning colloidal particles by an evaporative lithography technique.[274,275] A transparent conductive film was produced by placing a droplet containing gold NPs on top of a stainless-steel mesh placed on a glass substrate, followed by evaporation. During evaporation, the liquid flowed towards the metal wires of the mesh, leaving an empty area of the glass in each square of mesh. After complete evaporation, the mesh was removed and a transparent grid composed of the gold NPs was obtained. Sintering of the obtained pattern by heating at 425 °C for 20 min resulted in conductive gold grid with sheet resistance of 20 Ω/□ and transparency of 82% (**Figure 9**A).[276] Then, the obtained conductive network was transferred onto a plastic substrate by pressing on it a thin layer of UV hardening resin on a PET film followed by UV radiation (Figure 9B). To avoid transferring and post-printing sintering stages, PAA-stabilized silver NPs were deposited directly onto PET substrate, and the deposition was followed by RT sintering after exposure to HCl vapor. The process yielded a conductive array with sheet resistance of 9 Ω/□ and transparency above 75% in visible range.[250]

7.1.2. Metal Nanowires

Metal nanowires (NWs) are usually synthesized by the reduction of silver nitrate in presence of PVP in ethylene glycol.[69,71,72] Films composed of silver NWs are fabricated by various techniques, such as drop casting,[277–279]

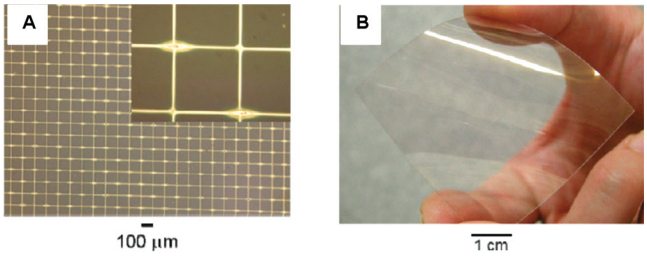

Figure 9. Gold network formed by Au NPs on glass plate sintered at 425 °C (A) and transparent Au grid transferred from glass onto PET film (B).Reproduced with permission.[276] Copyright 2011, American Chemical Society.

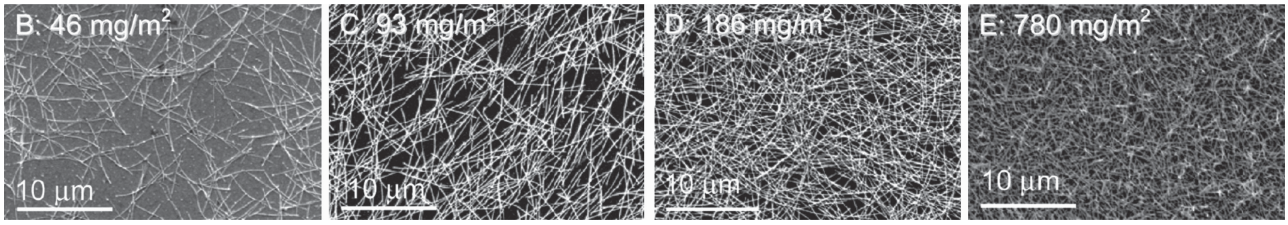

Figure 10. SEM images of silver NWs films of increasing thickness on Au/Pt glass. Reproduced with permission.[286] Copyright 2009, American Chemical Society.

spray-coating,[280,281] rod-coating,[282,283] (this method enables large-scale R2R coating on flexible substrates), spin-coating,[284] thermal nanoimprint lithography,[285] vacuum filtration followed by transfer printing,[286] and inkjet-printing.[287] The electrical conductivity and film transparency strongly depend on the thickness and post-deposition treatment, and for silver NWs are usually in the range of 10–100 Ω/□ and 80–90%, respectively,[279–282,284,288] that is comparable with ITO films.[8] The first conductive TEs based on silver NWs were fabricated by drop-casing onto a glass substrate followed by sintering at 200 °C for 20 min, and were characterized by sheet resistance in the range of 1–100 Ω/□ depending on coating density. **Figure 10** shows the SEM images of silver NWs with an average diameter of 84 nm and a length of 6.6 μm deposited onto Au/Pt coated glass. As seen, the increase in deposited mass per unit area resulted in the formation of films with increased density and homogeneity.[286] For the same NWs deposited onto PET substrate and heated to 100 ºC, the sheet resistance and transmittance were 13 Ω/□ and 85%, respectively, for film thickness of above 300 nm.[286]

Mixed gold/silver alloy NWs were grown by drying thin films containing a cationic surfactant, CTAB. Such films on silicon, quartz and PET were characterized by sheet resistance in the range of 60–1000 Ω/□ and by transmittance comparable to the transmittance of ITO films.[289]

A copper NWs film, formed by filtering aqueous dispersion of NWs onto a polycarbonate membrane, followed by imprinting onto a glass slide, yielded a film with sheet resistance of 15 Ω/□ and transmittance of 65%.[290] Transparent conductive films with improved characteristics were formed on PET by rod-coating a dispersion of copper NWs. The obtained films were treated with H_2/N_2 plasma and heated in H_2 atmosphere at 175 °C, yielding sheet resistance of 30–185 Ω/□ and transmittance of 85–90%, depending on the density of the coating.[291] NWs films composed of a Cu-Ni alloy were also formed by the same method on glass slides, showing transmittance of 84% and sheet resistance of 60 Ω/□.[291]

Recently, it has been reported that networks of copper nanofibers on glass slide (diameter of ~100 nm, length >100 μm) were obtained by the electrospinning method, yielding films with 200 and 50 Ω/□ at transparencies of 96 and 90% in the spectral range of 300–1100 nm.[292]

An important feature of NWs-based TEs is their stability under repeated bending and their retainment of conductivity.[279,280,283,284,286,289,290,292,293] For example, only ≤2% increase in sheet resistance was observed after 100–1000 cycles of bending films with silver and copper NWs.[283,286,290] In contrast, the sheet resistance of ITO films increased by 400 times after just 250 bends.[284]

Silver NWs-based flexible transparent conductors with sheet resistance in the range of 10–300 Ω/□ (ClearOhm material) produced by Cambrios Technologies (USA), were recently (2013) commercialized and are already replacing ITO films in flexible touch screens and displays in All-In-One computers of LG Electronics (Korea), large area monitors of eTurbotouch Technology (Taiwan), mobile phones of NEC/NTT Docomo (Japan), and kiosk monitors of G-Vision (USA). Electronic paper and flexible OLEDs are also getting close to mass production.[294]

7.1.3. Graphene

Fabrication of flexible transparent graphene films was performed by various methods: drop-casting,[295,296] dip-coating,[297] spin-coating,[298–302] spray-coating,[303] vacuum filtration followed by transferring onto a proper substrate,[176,180] electrophoretic deposition,[304,305] and inkjet printing.[44,45,49,306] As has been discussed in the previous sections, the sheet resistance of graphene films is thickness-dependent: increase in the number of deposited graphene layers results in a decrease in sheet resistance.[50,128,144,174,251] At the same time, increase in the film thickness leads to a decrease in its optical transparency in the visible range.[44,49,144] For example, graphene films inkjet printed onto poly(vinylidene fluoride) displayed sheet resistances of 700 and 10 kΩ/□ with corresponding light transmittances of ~90 and ~70% for film thicknesses of 30 and 60 nm, respectively.[306] Transmittances of about 80 and 88% and sheet resistances of 30 and 200 kΩ/□ (5 and 3 printed layers, respectively) were found for graphene films on glass slides.[44]

For flexible electronics, mechanical stability of printed devices is exceptionally important. The bending-relaxing experiments testify to the excellent stability of electrical parameters for graphene-based TEs on plastic substrates.[45,176,302] For example, the resistance of graphene film on PET varied not more than 6% from the initial value after 2000 cycles of bending.[176]

7.1.4. CNTs

Various methods, similar to those described above for graphene films obtaining, were also used for the preparation of flexible transparent CNT films: rod-coating,[257] spin-coating,[261,264] spray-coating,[8,254] dip-coating,[258] drop-casting,[307] vacuum filtration followed by transferring onto a

NANO MICRO small

proper substrate,[255] electrophoretic deposition followed by hot pressing transfer,[308] and inkjet printing.[23,186,191,200,202] As in the case of metal NWs and graphene sheets, both sheet resistance and transmittance are thickness-dependent, and CNT films with a thickness of 10–100 nm, possessing high electrical conductivity and optical transmittance, were reported.[8,24,36,267] Usually, SWCNTs are used for the fabrication of conductive transparent films, and electrical conductivity and transparency of such films on glass and plastic substrates are typically in the range of 60–870 Ω/□ and 70–90% respectively, depending on CNT dispersion, film thickness and method of preparation.[200,255,257,258,261,264,307]

Recently, highly conductive (4–24 Ω/□) films with 82% transparency were prepared, using a dispersion of silver NWs and SWCNTs by a vacuum filtration and transfer process. It was shown that the SWCNTs wrap around the Ag NWs, resulting in a conductive interconnect, as well as a mechanical support that provides structural integrity to the films.[309]

Because of the superior mechanical properties of individual CNTs and their strong interactions with hydrophobic substrates, thin films made of randomly distributed CNTs show excellent mechanical performance such as flexibility, stretchability, and foldability, which are important for flexible electronic devices and functional textile.[36] For example, only <0.5% increase in sheet resistance of SWCNT-based thin film on PET was observed after 2500 cycles of bending.[310]

At present, CNT films are at the market entry stage for application in touch screen sensors and flexible LEDs.[267]

7.2. RFID Tags

RFID (Radio Frequency Identification) tag is a device which provides storing and remote reading of data from items equipped with such tags. The main elements of an RFID tag are a silicon microchip and an antenna, which provide power to the tag and are responsible for communication with a reading device.[7,311] Direct inkjet printing of antennas on plastic and paper substrates with the use of metal NPs inks is a promising approach to the production of low-cost RFID tags. Since the antenna should be of low resistivity (the read distance depends on the antenna conductivity), silver and copper nanoparticulate inks are preferable. Appropriate processes for antenna printing with the use of such inks were reported.[7,26,29,216,245,311] However, to the best of our knowledge, metallic nanoinks are not used frequently in this field, probably due to the high cost of silver which is mainly commercially available. Recently, inkjet printing of graphene-based RFID antenna was demonstrated.[251]

7.3. Thin Film Transistors

Conductive nanomaterials are used to produce the conductive features on both inorganic and organic TFTs. For example, all-CNT TFTs were fabricated by controlled inkjet printing of SWCNT dispersions onto silicon wafer: the source and drain electrodes were obtained by deposition of dense SWCNT network (100 printed layers), while semiconducting films were obtained by deposition of 2 printed layers of SWCNT.[182] Organic TFTs were produced by inkjet printing of silver electrodes onto a pentacene film on PI and glass substrates, followed by sintering at 130–140 °C. The resistivity of the printed electrodes was $<2.5 \cdot 10^{-7}$ and $3 \cdot 10^{-7}$ Ω·cm, respectively.[312,313] Other silver electrodes printed onto SWCNT-based TFT had a sheet resistance of ~1 Ω/□ after post-printing sintering at 180 °C.[314] The applicability of mixed Ag-Cu NPs to print source/drain electrodes for poly(3-hexylthiophene)-based organic field-effect transistors was also demonstrated.[168] Recently, fabrication of source/drain electrodes by inkjet printing of inks composed of GO and PVA for flexible transparent organic field effect transistors was demonstrated.[315]

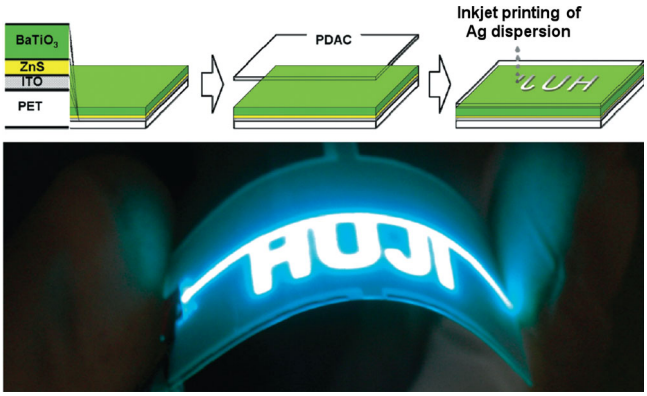

Figure 11. Top: Schematic illustration of ELD composition with an inkjet printed Ag electrode. Bottom: Working flexible ELD. Reproduced with permission.[244] Copyright 2010, American Chemical Society.

7.4. Light Emitting Devices

Light emitting devices (or electroluminescent devices, ELDs) are composed of a semiconductor layer placed between two electrodes, and emit light in response to electric current. LEDs to be used for lighting, require a highly conductive grid ("shunting lines") for homogeneous distribution of current around the lighting device.[1] These circuits can be fabricated on various substrates including plastic, by various printing processes using conductive nanomaterials. For example, silver electrodes were formed by inkjet printing a dispersion of silver NPs onto a four-layer flexible ELD. Applying voltage between the bottom ITO and the upper Ag electrodes resulted in intense (90 cd/sqm) emission of light (**Figure 11**).[244,256] In this process the sintering of the silver NPs was performed upon contact with a polycation, as described above. ELD with two CNT-printed electrodes was also recently fabricated, with the transparent back electrode made of a thin MWCNT film deposited by rod coating, and the counter electrode formed by inkjet printing. After applying a voltage between the two MWCNT electrodes, an intense emission was observed (**Figure 12**).[23,256] Recently, light emitting diode with inkjet printed graphene electrodes was also demonstrated.[252]

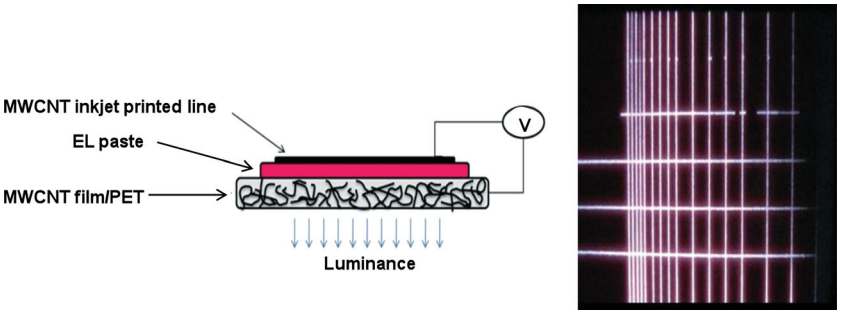

Figure 12. A scheme of flexible ELD with MWCNT electrodes (left) and a working device (right). Reproduced with permission.[23] Copyright 2012, IOP Publishing.

7.5. Solar Cells

Solar cells (SCs) are photovoltaic devices which convert solar radiation to electrical current. SCs are in fact large area semiconductor diodes based mainly on crystalline silicon (more than 85% of the world market). However, polycrystalline and amorphous silicon-based SCs, which are less efficient than the crystalline ones, are also widely used.[1] The electrical current is collected by metallic electrodes which are printed on the front side of the SCs. Currently such electrodes are produced by screen printing silver flakes with suitable additives, which enabled contact with the silicon. In recent years, metal NPs as well as NWs and CNTs have been also used in solar cells fabrication.[24,36] It is interesting to note that aluminum NPs may also be used, in spite of their rapid oxidation in air. To overcome this, the aluminum NPs, before printing onto Si, were etched with hexafluoroacetylacetone to remove the surface oxide layer.[316]

8. Outlook

As follows from the above overview, a number of nanomaterials of various chemical origins (metals, carbon) and morphologies (NPs, NWs, nanosheets, nanotubes) can be wet-deposited onto various substrates to obtain conductive patterns to be utilized in electronic and optoelectronic devices. In spite of the remarkable scientific progress in preparation processes and applications of conductive nanomaterials, they are still not widely used by the industry in significant quantities.

The current high price of commercially available inks, which are based mainly on the high cost silver, impedes their wide use for large area printed electronics. Therefore, research should be focused on the development of new nanomaterials and ink formulations based on low cost metals with high electrical conductivity such as copper, nickel, and aluminum. Such need requires overcoming the inherent surface oxidation of these metals by processes that can be performed on an industrial scale.

Since conductive patterning by metal inks on flexible plastic substrates and paper requires low-temperature sintering, further development of new sintering techniques, which are compatible with R2R printing processes (photonic, plasma, chemical etc.), is crucial to their application in plastic electronics, such as flexible displays and sensors.

Replacing traditional doped metal oxides (mainly ITO) used for transparent electrodes in many displays, by conductive nanomaterials, such as metal NPs, CNTs, and graphene can make a revolutionary impact on modern optoelectronics. Among the transparent conductive coatings, metal NWs-based inks are probably the most mature. Other reported approaches also seem to be very promising, while focusing on improving the wet deposition processes and film properties, such as stability and haze.[8]

Today, many research studies are directed towards conductive materials based on CNTs. Since the optoelectronic properties of CNT films are determined by numerous parameters (CNT purity, lattice perfection, aspect ratio, ratio of metallic, semiconducting CNTs, etc.), these parameters should be further optimized. For example, the development of new methods for scalable and cost effective separation of metallic and semiconducting CNTs, as well as direct synthesis of metallic CNTs, would enable simplified fabrication processes and better performance of printed devices.[8,36,267]

It should be noted that in recent years, many scientific activities have been focusing on graphene. Since graphene is an excellent conducting material, we can expect future developments in printed electronics that will combine CNTs with graphene. Successive utilization of graphene for printed electronics requires ink formulations with high graphene loading, which are stable against flakes aggregation.

One more important perspective in the application of conductive nanomaterials is 3D printing of conductive patterns. Nowadays, this field is at its very early stages of research and development, and the search for new nanomaterials as well as suitable 3D fabrication tools based on wet deposition, is a stimulating challenge for materials scientists.

Acknowledgements

This work was supported by NRF-Create "Nanomaterials for Energy and Water Management".

[1] A. Kamyshny, J. Steinke, S. Magdassi, *Open Appl. Phys. J.* **2011**, *4*, 19.
[2] M. M. Nir, D. Zamir, I. Haymov, L. Ben-Asher, O. Cohen, B. Faulkner, F. De La Vega, in Chemistry of Inkjet Inks (Ed.: S. Magdassi), World Scientific, New Jersey, London, Singapore, **2010**, pp. 225–254.
[3] M. Singh, H. M. Haverinen, P. Dhagat, G. E. Jabbour, *Adv. Mater.* **2010**, *22*, 673.
[4] J. Perelaer, U. S. Schubert, in Inkjet-Based Micromanufactoring (Eds: J. P. Korvink, P. J. Smith, D.-Y. Shin), Wiley-VCH, Weinheim, Germany **2012**, pp. 347–364.
[5] A. Sridhar, T. Blaudeck, R. R. Baumann, *Mater. Matters* **2011**, *6*, 1.

[6] G. Cummins, M. P. Y. Desmulliez, *Circuit Word* **2012**, *38*, 193.
[7] V. Subramanian, in Inkjet-Based Micromanufactoring (Eds: J. P. Korvink, P. J. Smith, D.-Y. Shin), Wiley-VCH, Weinheim, Germany **2012**, pp. 313–329.
[8] S. Park, M. Vosguerichiant, Z. Bao, *Nanoscale* **2013**, *5*, 1727.
[9] A. Rae, D. Hammer-Fritzinger, *Solid State Technology* **2006**, 53.
[10] S. Turner, *NSTI-Nanotech* **2011**, *2*, 558.
[11] A. Teichler, J. Perelaer, U. S. Schubert, *J. Mater. Chem. C* **2013**, *1*, 1910.
[12] A. Kamyshny, S. Magdassi, in Inkjet-Based Micromanufactoring (Eds: J. P. Korvink, P. J. Smith, D.-Y. Shin), Wiley-VCH, Weinheim, Germany **2012**, pp. 173–189.
[13] A. Hudd, in Chemistry of Inkjet Inks (Ed.: S. Magdassi), World Scientific, New Jersey, London, Singapore, **2010**, pp. 3–18.
[14] D. Wallace, in Inkjet-Based Micromanufactoring (Eds: J. P. Korvink, P. J. Smith, D.-Y. Shin), Wiley-VCH, Weinheim, Germany **2012**, 1–17.
[15] A. Kamyshny, S. Magdassi, in Nanoscience: Colloidal and Interfacial Aspects (Ed.: V. Starov), CRC Press, Boca Raton-London-New York, **2010**, pp. 747–778.
[16] A. Kamyshny, M. Ben-Moshe, S. Aviezer, S. Magdassi, *Macromol. Rapid Commun.* **2005**, *26*, 281.
[17] J. Perelaer, in Inkjet-Based Micromanufactoring (Eds: J. P. Korvink, P. J. Smith, D.-Y. Shin), Wiley-VCH, Weinheim, Germany **2012**, pp. 111–125.
[18] J. Perelaer, R. Jani, M. Grouchko, A. Kamyshny, S. Magdassi, U. S. Schubert, *Adv. Mater.* **2012**, *24*, 3993.
[19] M. Grouchko, A. Kamyshny, C. F. Mihailescu, D. F. Anghel, S. Magdassi, *ACS Nano* **2011**, *5*, 3354.
[20] F. M. Wolf, J. Perelaer, S. Stumpf, D. Bollen, F. Kriebel, U.S. Schubert, *J. Mater. Res.* **2013**, *28*, 1254.
[21] J. W. Song, Y. S. Kim, Y. H. Yoon, E. S. Lee, C. S. Han, Y. Cho, D. Kim, J. Kim, N. Lee, Y. G. Ko, H.T. Jung, S. H. Kim, *Physica E* **2009**, *41*, 1513.
[22] F. Torrisi, T. Hasan, W. Wu, Z. Sun, A. Lombardo, T. S. Kulmala, G-w. Hsieh, S. Jung, F. Bonaccorso, P. J. Paul, D. Chu, A. C. Ferrari, *ACS Nano* **2012**, *6*, 2992.
[23] S. Azoubel, S. Shemesh, S. Magdassi, *Nanotechnology* **2012**, *23*, 344003.
[24] D. S. Hecht, L. Hu, G. Irvin, *Adv. Mater.* **2011**, *23*, 1482.
[25] S. Magdassi, in Chemistry of Inkjet Inks (Ed.: S. Magdassi), World Scientific, New Jersey, London, Singapore, **2010**, pp. 19–41.
[26] M. Grouchko, A. Kamyshny, S. Magdassi, *Materials* **2010**, *3*, 4626.
[27] T. Campbell, R. K. Kalia, A. Nakano, P. Vashishta, *Phys. Rev. Lett.* **1999**, *82*, 4866.
[28] T. J. Foley, C. E. Johnson, K. T. Higa, *Chem. Mater.* **2005**, *17*, 4086.
[29] M. Grouchko, A. Kamyshny, S. Magdassi, *J. Mater. Chem.* **2009**, *19*, 3057.
[30] T. P. Ang, T. S. A. Wee, W. S. Chin, *J. Phys. Chem. B* **2004**, *108*, 11001.
[31] P. Kanninen, C. Johans, J. Merta, K. Kontturi, *J. Colloid Interface Sci.* **2008**, *318*, 88.
[32] S. Jeong, K. Woo, D. Kim, S. Lim, J. S. Kim, H. Shin, Y. Xia, J. Moon, *Adv. Funct. Mater.* **2008**, *18*, 679.
[33] Y. Lee, J. R. Choi, K. J. Lee, N. E. Stott, D. Kim, *Nanotechnology* **2008**, *19*, 415604.
[34] Y. Kobayashi, S. Ishida, K. Ihara, Y. Yasuda, T. Morita, S. Yamada, *Colloid Polym. Sci.* **2009**, *287*, 877.
[35] P. Pulkkinen, J. Shan, K. Leppanen, A. Kansakoski, A. Laiho, M. Jarn, H. Tenhu, *ASC Appl. Mater. & Interfaces* **2009**, *1*, 519.
[36] L. Hu, D. S. Hecht, G. Grüner, *Chem. Rev.* **2010**, *110*, 5790.
[37] A. Thess, R. Lee, P. Nikolaev, H. Dai, P. Petit, J. Robert, C. Xu, Y. H. Lee, S. G. Kim, A.G. Rinzler, D. T. Colbert, G. E. Scuseria, D. Tománek, J. E. Fischer, R. E. Smalley, *Science* **1996**, *273*, 483.
[38] H. Stahl, J. Appenzeller, R. Martel, P. Avoirus, B. Lengeler, *Phys. Rev. Lett.* **2000**, *85*, 5186.
[39] K. L. Lu, R. M. Lago, Y. K. Chen, M. L. H. Green, P. J. F. Harris, S. C. Tsang, *Carbon* **1996**, *34*, 814.
[40] D. A. Heller, P. W. Barone, M. S. Strano, *Carbon* **2005**, *43*, 651.
[41] S. Azoubel, S. Magdassi, *Carbon* **2010**, *48*, 3346.
[42] N. Behabtu, J. R. Lomeda, M. J. Green, A. L. Higginbotham, A. Sinitskii, D. V. Kosynkin, D. Tsentalovich, A. N. G. Parra-Vasques, J. Schmidt, E. Kesselman, Y. Cohen, Y. Talmon, J. M. Tour, M. Pasquali, *Nature Nanotechnol.* **2010**, *5*, 406.
[43] D. Parviz, S. Das, H. S. T. Ahmed, F. Irin, S. Bhattacharia, M. J. Green, *ACS Nano* **2013**, *6*, 8857.
[44] J. Li, F. Ye, S. Vaziri, M. Muhammed, M. C. Lemme, M. Östling, *Adv. Matter.* **2013**, *25*, 3985.
[45] L. Huang, Y. Huang, J. Liang, X. Wan, Y. Chen, *Nano Res.* **2011**, *4*, 675.
[46] Y. M. Jo, S. Yoon, J.-H. Lee, S.-J. Park, S. R. Kim, I. In, *Chem. Let.* **2011**, *40*, 54.
[47] L. T. Le, M. H. Ervin, H. Qiu, B. E. Fuchs, W. Y. Lee, *Electrochem. Commun.* **2011**, *13*, 355.
[48] F. J. Tölle, M. Fabritius, R. Mülhaupt, *Adv. Funct. Mater.* **2012**, *22*, 1136.
[49] D. Kong, L. T. Le, Y. Li, J. L. Zunino, W. Lee, *Langmuir* **2012**, *28*, 13467.
[50] C.-L. Lee, C.-H. Chen, C.-W. Chen, *Chem. Eng. J.* **2013**, *230*, 296.
[51] A. Henglein, *J. Phys. Chem.* **1993**, *97*, 5457.
[52] K. Kimura, in Fine Particles: Synthesis, Characterization, and Mechanism of Growth (Eds.: M. J. Schick, A. T. Hubbard), Marcel Dekker, New York-Basel, **2000**, pp. 513–550.
[53] Y. D. Tretyakov, A. V. Lukashin, A. A. Eliseev, *Russ. Chem. Rev.* **2004**, *73*, 899.
[54] Y. S. Kwon, A. A. Gromov, J. I. Strokova, *Appl. Surf. Sci.* **2007**, *253*, 5558.
[55] M. J. Pitkethly, *Nano Today* December 2004, *20*.
[56] F. Fiévet, in Fine Particles: Synthesis, Characterization, and Mechanism of Growth (Eds.: M. J. Schick, A. T. Hubbard), Marcel Dekker, New York-Basel, **2000**, pp. 460–496.
[57] N. Toshima, in Fine Particles: Synthesis, Characterization, and Mechanism of Growth (Eds.: M. J. Schick, A. T. Hubbard), Marcel Dekker, New York-Basel, **2000**, pp. 430–459.
[58] H. Bönneman, R. M. Richards, *Eur. J. Inorg. Chem.* **2001**, 2455.
[59] G. Schmid, in Nanoscale Materials in Chemistry (Ed.: K. J. Klabunde), John Wiley & Sons, New York, **2001**, pp. 15–59.
[60] A. Kamyshny, S. Magdassi, in Nanoparticles in Confined Structures: Formation and Application (Ed.: T. F. Tadros), Wiley-VCH, Weinheim, Germany, **2007**, pp. 207–233.
[61] L. N. Liz-Marzán, *Materials Today* **2004**, *7*, 26.
[62] Y. Sun, Y. Xia, *Analyst* **2003**, *128*, 686.
[63] D. V. Goia, *J. Mater. Chem.* **2004**, *14*, 451.
[64] L. Suber, I. Sondi, E. Matijević, D. V. Goia, *J. Colloid Interface Sci.* **2005**, *288*, 489.
[65] C. J. Murphy, T. K. Sau, A. M. Gole, *J. Phys. Chem. B* **2005**, *109*, 13857.
[66] M. S. Antelman, Chemical Electrode Potentials Plenum Press, New York-London, **1982**.
[67] X. F. Tang, Z. G. Yang, W. J. Wang, *Colloids Surf. A* **2010**, *360*, 99.
[68] F. Bonet, V. Delmas, S. Grugeon, R. Herrera Urbina, P.-Y. Silvert, K. Tekaia-Elhsissen, *Nanostruct. Mater.* **1999**, *11*, 1277.
[69] B. Wiley, Y. Sun, B. Mayers, Y. Xia, *Chem. Eur. J.* **2005**, *11*, 454.
[70] H. Hei, H. He, R. Wang, X. Liu, G. Zhang, *Soft Nanosci. Lett.* **2012**, *2*, 34.
[71] Y. Sun, Y. Xia, *Adv. Mater.* **2002**, *14*, 833.
[72] X. Tang, M. Tsuji, in Nanowires Science and Technology (Ed: N. Lupu), InTech, Rijeka, Croatia, Shanghai, China, **2010**, pp. 25–42.
[73] S. Jeong, H. C. Song, W. W. Lee, S. S. Lee, Y. Choi, W. Son, E. D. Kim, C. H. Paik, S. H. Oh, B. H. Ryu, *Langmuir* **2011**, *27*, 3144.

[74] M. Starowicz, B. Stypuła, J. Banaś, *Electrochem. Commun.* **2006**, *8*, 227.
[75] M. Raja, J. Shuba, F. B. Ali, S. H. Ryu, *Mater. Manufact. Process* **2008**, *23*, 782.
[76] J. Cheon, J. Lee, J. Kim, *Thin Solid Films* **2012**, *520*, 2639.
[77] N. A. Dhas, C. P. Raj, A. Gedanken, *Chem. Mater.* **1998**, *10*, 1446.
[78] G. W. Yang, H. Li, *Mater. Lett.* **2008**, *62*, 2189.
[79] J. Zhu, S. Liu, O. Palchik, Y. Koltypin, A. Gedanken, *Langmuir* **2000**, *16*, 6396.
[80] I. Haas, S. Shanmugam, A. Gedanken, *J. Phys. Chem. B* **2006**, *110*, 16947.
[81] S. Kapoor, *Langmuir* **1998**, *14*, 1021.
[82] S. Kapoor, *Langmuir* **1999**, *15*, 4365.
[83] A. Henglein, M. Giersig, *J. Phys. Chem. B* **1999**, *103*, 9533.
[84] J.-T. Lee, S.-Y. Heo, M.-S. Kim, H.-S. Kim, *Intern. Patent Appl.* **2008**, WO 2008/038867.
[85] I. Okada, K. Shimada, US Papent 7,608,203, **2009**.
[86] D. Kim, S. Jeong, B. K. Park, J. Moon, *Appl. Phys. Lett.* **2006**, *89*, 264101.
[87] S. Jeong, K. Woo, D. Kim, S. Lim, J. S. Kim, H. Shin, Y. Xia, J. Moon, *Adv. Func. Mater.* **2008**, *18*, 679.
[88] J. S. Kim, J. H. Moon, S. H. Jeong, D. J. Kim, B. K. Park, **2007**, *US Patent Appl*. 2007/0180954.
[89] X. Li, Y. Li, P. B. Laxton, D. M. Roundhill, H. Arimura, **2009**, *US Patent Appl*. **2009**/0242854.
[90] K-S. Chou, Y-S. Lai, *Mater. Chem. Phys.* **2004**, *83*, 82.
[91] H-H. Lee, K. Chou, K-C. Huang, *Nanotechnology* **2005**, *16*, 2436.
[92] J.-S. Chang, Y.-P. Lee, R.-C. Wang, *Ind. Eng. Chem. Res.* **2007**, *46*, 5591.
[93] R. Patakfalvi, S. Papp, I. Dékány, *J. Nanopart. Res.* **2007**, *9*, 353.
[94] A. Sarkar, T. Mukherjee, S. Kapoor, *J. Phys. Chem. C* **2008**, *112*, 3334.
[95] D. Kim, J. Moon, *Electrochem. Solid-State Lett.* **2005**, *8*, J30.
[96] B. K. Park, D. Kim, S. Jeong, J. Moon, J. S. Kim, *Thin Solid Films* **2007**, *515*, 7706.
[97] B. K. Park, S. Jeong, D. Kim, J. Moon, S. Lim, J. S. Kim, *J. Colloid Interface Sci.* **2007**, *311*, 417.
[98] K. Woo, D. Kim, J. S. Kim, S. Lim, J. Moon, *Langmuir* **2009**, *25*, 429.
[99] K. K. Toshiba, *Eur. Patent Appl.* **2011**, *EP 2441922*.
[100] S. Ummartyotin, N. Bunnak, J. Juntaro, M. Sain, H. Manuspiya, *Compt. Rend. Chim.15*, 539.
[101] T. Teranishi, M. Miyake, *Chem. Mater.* **1998**, *10*, 594.
[102] B.-H. Ruy, Y. Choi, H.-S. Park, J.-H. Byun, K. Kong, J.-O. Lee, H. Chang, *Colloids Surf A* **2005**, *270–271*, 345.
[103] M. Grouchko, A. Kamyshny, K. Ben-Ami, S. Magdassi, *J. Nanopart. Res.* **2009**, *11*, 713.
[104] S. Magdassi, A. Bassa, Y. Vinetsky, A. Kamyshny, *Chem. Mater.* **2003**, *15*, 2208.
[105] H. Chen, Y. Wang, Y. Wang, S. Dong, E. Wang, *Polymer* **2006**, *47*, 763.
[106] X. Sun, S. Dong, E. Wang, *Polymer* **2004**, *45*, 2181.
[107] S. Magdassi, A. Kamyshny, S. Aviezer, M. Grouchko, US Patent Appl. **2012**, 20120241693.
[108] Y. Wang, P. Chen, M. Liu, *Nanotechnology* **2006**, *17*, 6000.
[109] K. Woo, C. Bae, Y. Jeong, D. Kim, J. Moon, *J. Mater. Chem.* **2010**, *20*, 3877.
[110] D. Mott, J. Galkowski, L. Wang, J. Luo, C.-J. Zhong, *Langmuir* **2007**, *23*, 5740.
[111] S. Jeong, S. H. Lee, Y. Jo, S. S. Lee, Y.-H. Seo, B. W. Ahn, G. Kim, G.-E. Jang, J.-U. Park, B.-H. Ryu, Y. Choi, *J. Mater. Chem. C* **2013**, *1*, 2704.
[112] X. Song, S. Sun, W. Zhang, Z. Yin, *J. Colloid Interface Sci.* **2004**, *273*, 463.
[113] T. P. Ang, T. S. A. Wee, W. S. Chin, *J. Mater. Chem.* **2012**, *22*, 23989.
[114] V. Engels, F. Benaskar, D. A. Jefferson, B. F. G. Johnson, A. E. H. Wheatley, *Dalton Trans.* **2010**, *39*, 6496.
[115] S.-H. Wu, D.-H. Chen, *J. Colloid Interface Sci.* **2004**, *273*, 165.
[116] D. Deng, Y. Cheng, Y. Jin, T. Qi, F. Xiao, *J. Mater. Chem.* **2012**, *22*, 23989.
[117] I. Kim, Y. Kim, K. Woo, E.-H. Ryu, K.-Y. Yon, G. Cao, J. Moon, *RSC Adv.* **2013**, *3*, 15169.
[118] C. Wu, B. P. Mosher, T. Zeng, *J. Nanopart. Res.* **2006**, *8*, 965.
[119] N. A. Leuchinger, E. K. Athanassiou, W. J. Stark, *Nanotechnology* **2008**, *19*, 445201.
[120] N. Toshima, T. Yonezawa, *New J. Chem.* **1998**, *22*, 1179.
[121] M. Sastry, A. Swami, S. Mandal, Pr. Selvacannan, *J. Mater. Chem.* **2005**, *15*, 3161.
[122] W. Lee, M. G. Kim, J. Choi, J. Park, S. J. Ko, S. J. Oh, J. Cheon, *J. Am. Chem. Soc.* **2005**, *127*, 16090.
[123] D. Chen, J. Li, C. Shi, X. Du, N. Zhao, J. Sheng, S. Liu, *Chem. Mater.* **2007**, *19*, 3399.
[124] S. Magdassi, M. Grouchko, A. Kamyshny, *Intetrn. Patent Appl.* **2009**, *WO 2009/156990*.
[125] C.-H. Tsai, S.-Y. Chen, J.-M. Song, I.-G. Chen, H.-Y. Lee, *Corrosion Sci.* **2013**, *74*, 123.
[126] A. K. Geim, K. S. Novoselov, *Nature Mater.* **2007**, *6*, 183.
[127] F. Tian, A. Konar, X. Huili, D. Jena, *Appl. Phys. Lett.* **2007**, *91*, 092109.
[128] B. Wu, M. Agrawal, H. A. Becerril, Z. N. Bao, Z. F. Liu, Y. S. Chen, P. Peumans, *ACS Nano* **2010**, *4*, 43.
[129] K. S. Novoselov, A. K. Geim, S. V. Morozov, D. Jiang, Y. Zhang, S. V. Dubonos, I. V. Grigorieva, A. A. Firsov, *Science* **2004**, *306*, 666.
[130] Y. Hernandez, V. Nicolisi, M. Lotya, F. M. Blighe, Z. Sun, S. De, I. T. McGovern, B. Holland, M. Byrne, Y. K. Gun'ko, J. J. Boland, P. Niraj, G. Duesberg, S. Krishnamurthy, R. Goodhue, J. Hutchison, V. Scardaci, A. C. Ferrari, J. N. Coleman, *Nature Nanotechnol.* **2008**, *3*, 563.
[131] M. Lotya, Y. Hernandez, P. J. King, R. J. Smith, V. Nicoloci, L. S. Karlsson, F. M. Blighe, S. De, Z. Wang, I. T. McGovern, G. S. Duesberg, J. N. Coleman, *J. Am. Chem. Soc.* **2009**, *131*, 3611.
[132] C. Vallés, C. Drummomd, H. Saadaoui, C. A. Furtado, M. He, O. Roubeau, L. Ortolani, M. Monthioux, A. Pénicaud, *J. Am. Chem. Soc.* **2008**, *130*, 15802.
[133] T. Hasan, F. Torrisi, Z. Sun, D. Popa, V. Nicolosi, G. Privitera, F. Bonaccorso, A. C. Ferrari, *Phys. Status Solidi B* **2010**, *247*, 2953.
[134] K. S. Kim, Y. Zhao, H. Jang, S. Y. Lee, J. M. Kim, K. S. Kim, J.-H. Ahn, P. Kim, J.-Y. Choi, B. H. Hong, *Nature* **2009**, *457*, 706.
[135] A. Reina, x. Jia, J. Ho Nezich, H. Son, V. Bulovic, M. S. Dresselhaus, J. Kong, *Nano Lett.* **2009**, *9*, 30.
[136] X. S. Li, W. W. Cai, J.-H. An, S. Kim, J. Nah, D. X. Yang, R. Piner, A. Velamakanni, I. Jung, E. Tutuc, S. K. Banerjee, L. Colombo, R. S. Ruoff, *Science* **2009**, *324*, 1312.
[137] M. Choucair, P. Thordarson, J. A, Stride, *Nature Nanotechnol.* **2009**, *4*, 30.
[138] X. Wang, L. Zhi, N. Tsao, Ž. Tomori, J. Li, K. Müllen, *Angew. Chem. Int. Ed.* **2008**, *47*, 2990.
[139] C. Berger, Z. Song, T. Li, X. Li, A. Y. Orbazghi, R. Feng, Z. Dai, A. N. Marchenkov, E. H. Conrad, P. N. First, W. A. De Heer, *J. Phys. Chem. B* **2004**, *108*, 19912.
[140] K. V. Emtsev, A. Bostwick, K. Hom, J. Jobst, G. L. Kellog, L. Ley, J. L. McChesney, T. Ohta, S. A. Reshanov, J. Röhrl, E. Rotenberg, A. S. Schmid, D. Waldmann, H. B. Weber, T. Seyller, *Nature Mater.* **2009**, *8*, 203.
[141] B. Dai, L. Fu, L. Liao, N. Liu, K. Yan, Y. Chen, Z. Liu, *Nano Res.* **2011**, *4*, 434.
[142] S. Wang, P. K. Ang, Z. Wang, A. L. L. Tang, J. T. L. Thong, K. P. Loh, *Nano Lett.* **2010**, *10*, 92.
[143] D. Wei, H. Li, D. Han, Q. Zhang, L. Niu, H. Yang, C. Bower, P. Andrew, T. Ryhanen, *Nanotechnology* **2011**, *22*, 245702.

[144] G. Eda, M. Chhowalla, *Adv. Mater.* **2010**, *22*, 2392.
[145] P. L. McEuen, M. Fuhrer, H. Park, *IEEE Trans. Nanotechnol.* **2002**, *2*, 78.
[146] A. Bachtold, M. Henny, C. Terrier, C. Strunk, L. Forro, *Appl. Phys. Lett.* **1998**, *73*, 274.
[147] Q. Li, Y. Li, X. Zhang, S. B. Chikkannanavar, Y. Zhao, A. M. Dangelewicz, L. Zheng, S. K. Doorn, Q. Jia, D. E. Peterson, P. N. Arendt, Y. Zhu, *Adv. Mater.* **2007**, *19*, 3358.
[148] M. Terrones, *Annu. Rev. Mater. Res.* **2003**, *33*, 419.
[149] A. Szabó, C. Perri, A. Csató, G. Giordano, D. Vuono, J. B. Nagy, *Marterials* **2010**, 3092.
[150] J. Prasek, J. Drbohlavova, J. Chomoucka, J. Hubalek, O. Jasek, V. Adam, R. Kizek, *J. Mater. Chem.* **2011**, *21*, 15872.
[151] Y. C. Liu, N. N. Zheng, J. D. Huang, B. M. Sun, in Advanced Polymer Science and Engineering (Eds.: C. H. Wang, L. X. Ma, W. Yang), Trans Tech Publications, Durnten-Zurich, Switzerland **2011**, pp. 99–103.
[152] R. Jasti, C. R. Bertozzi, *Chem. Phys. Lett.* **2010**, *494*, 1.
[153] Y. Gogotsi, J. A. Libera, M. Yoshimura, *J. Mater. Res.* **2000**, *15*, 2591.
[154] Y. Gogotsi, N. Naguib, J. A. Libera, *Chem. Phys. Lett.* **2002**, *365*, 354.
[155] B.-H. Ryu, Y. Choi, H.-S. Park, J.-H. Byun, K. Kong, J.-O. Lee, H. Chang, *Colloids Surf. A* **2005**, *270–271*, 345.
[156] J. G. Bai, K. D. Creehan, H. A. Kuhn, *Nanotechnology* **2007**, *18*, 185701.
[157] K. Balantrapu, D. V. Goia, *J. Mater. Res.* **2009**, *24*, 2828.
[158] T. H. Kim, Y. K. Seo, D. H. Kim, B. H. Jun, S. E. Kim, *US Patent Appl.* **2009**, *US 2011/0318541*.
[159] Z. Zhang, X. Zhang, Z. Xin, M. Deng, Y. Wen, Y. Song, *Nanotechnology* **2011**, *22*, 425601.
[160] I. Jung, Y. H. Jo, I. Kim, H. M. Lee, *J. Electron. Mater.* **2012**, *41*, 115.
[161] J.-W. Joung, Y.-S. Oh, I.-K. Shim, *US Patent* **2009**, No. 7611644.
[162] F. Mafune, J. Kohno, Y. Takeda, T. Kondow, *J. Phys. Chem. B* **2000**, *104*, 9111.
[163] Y.-H. Chen, C.-S. Yeh, *Colloids Surf. A* **2002**, *197*, 133.
[164] J. Keskinen, P. Ruuskanen, M. Karttunen, S.-P. Hannula, *Appl. Organomet. Chem.* **2001**, *15*, 393.
[165] J. Lee, J.-G. Ahn, L. M. Tung, D.-J. Kim, C.-O. Kim, H. S. Chung, B.-G. Kim, *TMS Lett.* **2006**, *3*, 41.
[166] C. O. Oriakhi, *US Patent* **2009**, No. 7615111.
[167] J. B. Szczech, C. M. Megaridis, J. Zhang, D. R. Gamota, *Microscale Thermophys. Eng.* **2004**, *8*, 327.
[168] S. Gamerith, A. Klug, H. Scheiber, U. Scherf, E. Moderegger, E. J. W. List, *Adv. Func. Mater.* **2007**, *17*, 3111.
[169] D. Itoh, A. Izumitani, N. Hata, Y. Matsuba, K. Murata, H. Yokoyama, *Eur. Pat. Appl.* **2006**, EP 1 666 175.
[170] Y. Li, J. S.-C. Lee, H. Pan, P. F. Smith, H. K. Mahabadi, *US Patent Appl.* **2009**,2009/0148600.
[171] S. B. Fuller, E. J. Wilhelm, J. M. Jacobson, *J. Microelectromech. Syst.* **2002**, *11*, 54.
[172] K.-C. Chung, H.-N. Cho, M.-S. Gong, Y.-S. Han, J.-B. Park, D.-H. Nam, S.-Y. Uhm, Y.-K. Seo, N.-B. Cho, *US Patent Appl.* **2008**, 2008/0206488.
[173] C.-C. Tseng, C.-P. Chang, Y. Sung, Y.-C. Chen, M.-D. Ger, *Colloids Surf. A* **2009**, *339*, 206.
[174] E. B. Secor, P. L. Prabhumirashi, K. Puntambekar, M. L. Geier, M. C. Hersam, *J. Phys. Chem. Lett.* **2013**, *4*, 1347.
[175] A. A. Green, M. C. Hersam, *Nano Lett.* **2009**, *9*, 4031.
[176] S. De, P. J. King, M. Lotya, A. O'Neil, E. M. Doherty, Y. Hernandez, G. G. Duesberg, J. N. Coleman, *Small* **2010**, *6*, 458.
[177] S. Vadukumpully, J. Paul, S. Valiyaveettil, *Carbon* **2009**, *47*, 3288.
[178] A. S. Wajid, S. Das, F. Irin, H. S. T. Ahmed, J. L. Shelburne, D. Parviz, R. J. Fullerton, A. F. Jankowski, R. C. Hedden, *Carbon* **2012**, *50*, 526.
[179] S. Das, F. Irin, H. S. T. Ahmed, A. B. Cortinas, A. S. Wajid, D. Parviz, A. F. Jankowski, M. Kato, M. J. Green, *Polymer* **2012**, *53*, 2485.
[180] G. Eda, G. Fanchini, M. Chhowalla, *Nature Nanotechnol.* **2008**, *3*, 270.
[181] J. I. Paredes, S. Villar-Rodil, A. Martínez-Alonso, J. M. D. Tascón, *Langmuir* **2008**, *24*, 10560.
[182] H. Okimoto, T. Takenobi, K. Yanagi, Y. Miyata, H. Shimotani, H. Kataura, Y. Iwasa, *Adv. Mater.* **2010**, *22*, 3981.
[183] J.-W. Song, J. Kim, Y.-H. Yoon, B.-S. Choi, J.-H. Kim, C.-S. Han, *Nanotechnology* **2008**, *19*, 095702.
[184] P. Beecher, P. Servati, A. Rozhin, A. Colli, V. Scardaci, S. Pisana, T. Hasan, A. J. Flewitt, J. Robertson, G. W. Hsieh, F. M. Li, A. Nathan, A. C. Ferrari, W. I. Milne, *J. Appl. Phys.* **2007**, *102*, 043710.
[185] J. Fan, T. Wei, G. Luo, F. Wei, *J. Mater. Sci.* **2005**, *40*, 5075.
[186] W. R. Small, M. in het Panhius, *Small* **2007**, *3*, 1500.
[187] R. Rastogi, R. Kaushal, S. K. Tripathi, A. L. Sharma, I. Kaur, L. M. Bharadwaj, *J. Colloid Interface Sci.* **2008**, *328*, 421.
[188] M. Mionić, K. Pataky, R. Gaal, A. Magrez, J. Brugger, L. Forró, *J. Mater. Chem.* **2012**, *22*, 14030.
[189] S. T. Beyer, K. Walus, *Langmuir* **2012**, *28*, 8753.
[190] L. B. Robertson, M. K. Williams, T. L. Gibson, L. C. Tate, S. J. Snyder, C. R. Fortier, *US Patent Appl.* **2012**, 2012/0111599.
[191] K. Kordás, T. Mustonen, G. Tóth, H. Jantunen, M. Lajunen, C. Soldano, S. Talapatra, S. Kar, R. Vajtai, P. M. Ajayan, *Small* **2006**, *2*, 1021.
[192] A. Denneulin, J. Bras, F. Carcone, C. Neuman, A. Blayo, *Carbon* **2011**, 2603.
[193] M. F. Islam, E. Rojas, D. M. Bergey, A. T. Johnson, A.G. Yodh, *Nano Lett.* **2003**, *3*, 269.
[194] H. Wang, W. Zhou, D. L. Ho, K. I. Winey, J. E. Fischer, C. J. Glinka, E. K. Hobbie, *Nano Lett.* **2004**, *4*, 1789.
[195] E. A. Whisitt, A. R. Barron, *Nano Lett.* **2003**, *3*, 775.
[196] J. Yu, N. Grossiord, C. E. Koning, J. Loos, *Carbon* **2007**, *45*, 618.
[197] A. G. Ryabenko, T. V. Dorofeeva, G. I. Zvereva, *Carbon* **2004**, *42*, 1523.
[198] T. Panagiotou, J. M. Bernard, S. V. Mesite, *NSTI-Nanotech.* **2008**, *1*, 39.
[199] V. A. Davis, A. N. G. Parra-Vasquez, M. J. Green, P. K. Rai, N. Behabtu, V. Prieto, R. D. Booker, J. Schmidt, E. Kesselman, W. Zhou, H. Fan, W. W. Adams, R. H. Hauge, J. E. Fischer, Y. Cohen, Y. Talmon, R. E. Smalley, M. Pasquali, *Nature Nanotechnol.* **2009**, *4*, 830.
[200] Y.-I. Lee, S. Kim, K.-J. Lee, N. V. Myung, Y.-H. Choa, *Thin Solid Films* **2013**, *536*, 160.
[201] J. Samurel, *US Patent Appl.* **2012**, 2012/0141678.
[202] T. Wei, J. Ruan, Z. Fan, G. Luo, F. Wei, *Carbon* **2007**, *45*, 2712.
[203] R. Ma, D. Suh, J. Kim, J. Chung, S. Baik, *J. Mater. Chem.* **2011**, *21*, 7070.
[204] D. Zhao, T. Liu, J. G. Park, M. Zhang, J.-M. Chen, B. Wang, *Microelectron. Eng.* **2012**, *96*, 71.
[205] T. Mustonen, K. Kordás, S. Saukko, G. Tóth, J. S. Pantilä, P. Helistö, H. Seppä, H. Jantunen, *Phys. Stat. Sol.* **2007**, *244*, 4336.
[206] C. K. Najeeb, J.-H. Lee, J. Chang, J.-H. Kim, *Nanotechnology* **2010**, *21*, 385302.
[207] S. H. Ko, J. Chung, N. Hotz, K. H. Nam, C. P. Grigoropoulos, *J. Micromech. Microeng.* **2010**, *20*, 125010.
[208] C. Kullmann, N. C. Schirmer, M.-T. Lee, S. H. Ko, N. Hotz, C. P. Grigoropoulos, D. Poulikakos, *J. Micromech. Microeng.* **2012**, *22*, 055022.
[209] E. Napadensky, in Chemistry of Inkjet Inks (Ed.: S. Magdassi), World Scientific, New Jersey, London, Singapore, **2010**, pp. 255–267.
[210] M. Sangermano, A. Chiolerio, G. Marti, P. Martino, *Macromol. Mater. Eng.* **2013**, *298*, 607.

[211] M. Layani, I. Cooperstein, S. Magdassi, *J. Mater. Chem. C* **2013**, *1*, 3244.
[212] Ph. Buffat, J.-P. Borel, *Phys. Rev. A* **1976**, *13*, 2287.
[213] K. Dick, T. Dhanasekaran, Z. Zhang, D. Meisel, *J. Am. Chem. Soc.* **2002**, *124*, 2312.
[214] J. Perelaer, P. J. Smith, D. Mager, D. Soltman, S. K. Volkman, V. Subramanian, J. G. Korvnik, U. S. Schubert, *J. Mater. Chem.* **2010**, *20*, 8446.
[215] A. Scandurra, G. F. Indelli, N. G. Spartà, F. Galliano, S. Ravesi, S. Pignataro, *Surf. Interface Anal.* **2010**, *42*, 1163.
[216] M. L. Allen, K. Jaakkola, K. Nummila, H. Seppa, *IEEE Trans. Comp. Packag. Technol.* **2009**, *32*, 325.
[217] J. S. Kang, H. S. Kim, J. Ryu, H. T. Hahn, S. Jang, J. W. Joung, *J. Mater. Sci.* **2010**, *21*, 1213.
[218] A. Khan, K. Rahman, D. S. Kim, K. H. Choi, *J. Mater. Proc. Technol.* **2012**, *212*, 700.
[219] D. Huang, F. Liao, S. Molesa, D. Redinger, V. Subramanian, *J. Electrochem. Soc.* **2003**, *150*, G412.
[220] J. Perelaer, A. W. M. De Laat, C. E. Hendriks, U. S. Schubert, *J. Mater. Chem.* **2008**, *18*, 3209.
[221] S. Joo, D. F. Baldwin, *Nanotechnology* **2010**, *21*, 055204.
[222] S. Jeong, H. C. Song, W. W. Lee, Y. Choi, S. S. Lee, B-H. Ryu, *J. Phys. Chem. C* **2010**, *114*, 22277.
[223] D. Jang, D. Kim, B. Lee, S. Kim, M. Kang, D. Min, J. Moon, *Adv. Func. Mater.* **2008**, *18*, 2862.
[224] K. C. Yung, X. Gu, C. P. Lee, H. S. Choy, *J. Mater. Proc. Technol.* **2010**, *210*, 2268.
[225] D. J. Lee, S. H. Park, S. Jang, H. S. Kim, J. H. Oh, Y. W. Song, *J. Micromech. Microeng.* **2011**, *21*, 125023.
[226] Advanced curing for printed electronics. Available from: http://www.novacentrix.com/ images/downloads/PF_Brochure_4pg.pdf.
[227] H.-S. Kim, S. R. Dhage, D.-E. Shim, H. T. Hahn, *Appl. Phys.* **2009**, *97*, 791.
[228] J. S. Kang, J. Ryu, H. S. Kim, H. T. Hahn, *J. Electron. Mater.* **2011**, *40*, 2268.
[229] D. Tobjörk, H. Aarnio, P. Pulkkinen, R. Bollström, A. Määttänen, P. Ihalainen, T. Mäkelä, J. Peltonen, M. Toivakka, H. Tenhu, R. Österbacka, *Thin Solid Films* **2012**, *520*, 2949.
[230] M. Hösel, F. C. Krebs, *J. Mater. Chem.* **2012**, *22*, 15683.
[231] J. Chung, S. Ko, N. R. Bieri, C. P. Grigoropoulos, D. Poulikakos, *Appl. Phys. Lett.* **2004**, *84*, 801.
[232] N. R. Bieri, J. Chung, D. Poulikakos, C. P. Grigoropoulos, *Superlattices and Microstruct.* **2004**, *35*, 437.
[233] S. H. Ko, H. Pan, C. P. Grigoropoulos, C. K. Luscombe, J. M. J. Fréchet, D. Poulikakos, *Nanotechnology* **2007**, *18*, 345202.
[234] K. Maekawa, K. Yamasaki, T. Niizeki, M. Mita, Y. Matsuba, N. Terada, H. Saito, *IEEE Trans. Comp. Packag. Manufactur. Technol.* **2012**, *2*, 868.
[235] Z. Cai, K. C. Yung, X. Zeng, *Appl. Surf. Sci.* **2011**, *258*, 478.
[236] J. Perelaer, U. S. Schubert, *J. Mater. Res.* **2013**, *28*, 564.
[237] I. Reinhold, C. E. Hendriks, R. Eckardt, J. M. Kranenburg, J. Perelaer, R. R. Baumann, U. S. Schubert, *J. Mater. Chem.* **2009**, *19*, 3384.
[238] S. Wünscher, S. Stumpf, A. Teichler, O. Pabst, J. Perelaer, E. Beckert, U. S. Schubert, *J. Mater. Chem.* **2012**, *22*, 24569.
[239] J. Perelaer, B.-J. de Gans, U. S. Schubert, *Adv. Mater.* **2006**, *18*, 2101.
[240] J. Perelaer, M. Klokkenburg, C. E. Hendriks, U. S. Schubert, *Adv. Mater.* **2009**, *21*, 4830.
[241] J. Perelaer, R. Abbel, S. Wünscher, R. Jani, T. van Lammeren, U. S. Schubert, *Adv. Mater.* **2012**, *24*, 2620.
[242] M. L. Allen, M. Aronniemi, T. Mattila, A. Alastalo, K. Ojanperä, M. Suhonen, H. Seppä, *Nanotechnology* **2008**, *19*, 175201.
[243] A. T. Alastalo, T. Mattila, M. L. Allen, M. J. Aronniemi, J. H. Leppäniemi, K. A. Ojanperä, M. P. Suhonen, H. Seppä, *Mater. Res. Soc. Symp. Proc.* **2009**, *1113*, 1113-F02–07.
[244] S. Magdassi, M. Grouchko, O. Berezin, A. Kamyshny, *ACS Nano* **2010**, *4*, 1943.
[245] S. Magdassi, M. Grouchko, A. Kamyshny, *NIP25: Intern. Conf. on Digital Printing Technologies and Digital Fabrication, Proceeding* **2009**, 611.
[246] M. J. Coutts, M. B. Cortie, M. J. Ford, A. M. McDonagh, *J. Phys. Chem. C* **2009**, *113*, 1325.
[247] W. Zapka, W. Voit, C. Loderer, P. Lang, *NIP24: Intern. Conf. on Digital Printing Technologies and Digital Fabrication, Proceeding* **2008**, 906.
[248] Y. Tang, W. He, G. Zhou, S. Wang, X. Yang, Z. Tao, J. Zhou, *Nanotechnology* **2012**, *23*, 355304.
[249] M. Layani, M. Grouchko, S. Shemesh, S. Magdassi, *J. Mater. Chem.* **2012**, *22*, 14349.
[250] M. Layani, S. Magdassi, *J. Mater. Chem.* **2011**, *21*, 15378.
[251] K.-Y. Shin, J.-Y. Hong, J. Jang, *Adv. Mater.* **2011**, *23*, 2113.
[252] K. Kim, S. I. Ahn, K. C. Choi, *Carbon* **2014**, *66*, 172.
[253] R. Jackson, B. Domercq, R. Jain, B. Kippelen, S. Graham, *Adv. Funct. Mater.* **2008**, *18*, 2548.
[254] P. N. Nirmalraj, P. E. Lyons, S. De, J. N. Coleman, J. J. Boland, *Nano Lett.* **2009**, *9*, 3890.
[255] D. S. Hecht, A. M. Heintz, R. Lee, L. Hu, B. Moore, C. Cucksey, S. Risser, *Nanotechnology* **2011**, *22*, 075201.
[256] S. Magdassi, S. Azoubel, M. Layani, M. Grouchko, A. Kamyshny, *NIP28: Intern. Conf. on Digital Printing Technologies and Digital Fabrication, Proceeding* **2012**, 561.
[257] B. Dan, G. C. Irvin, M. Pasquali, *ACS Nano* **2009**, *3*, 835.
[258] N. Saran, K. Parikh, D.-S. Suh, E. Muños, H. Kolla, S. K. Manohar, *J. Am. Chem. Soc.* **2004**, *126*, 4462.
[259] B. B. Parekh, G. Fanchini, G. Eda, M. Chhowalla, *Appl. Phys. Lett.* **2007**, *90*, 121913.
[260] H.-Z. Geng, K. K. Kim, K. P. So, Y. S. Lee, Y. Chang, Y. H. Lee, *J. Am. Chem. Soc.* **2007**, *129*, 7758.
[261] S. L. Hellstrom, H. W. Lee, Z. Bao, *ACS Nano* **2009**, *3*, 1423.
[262] D.-W. Shin, J. H. Lee, Y.-H. Kim, S. M. Yu, S.-Y. Park, J.-B. Yoo, *Nanotechnology* **2009**, *20*, 475703.
[263] S. Manivannan, J. H. Ryu, H. E. Lim, M. Nakamoto, J. Jang, K. C. Park, *J. Mater. Sci.: Mater. Electron.* **2010**, *21*, 72.
[264] J. W. Jo, J. W. Jung, J. U. Lee, W. H. Jo, *ACS Nano* **2010**, *4*, 5382.
[265] Y. Zhao, W. Li, *Microelectron. Eng.* **2010**, *87*, 576.
[266] J. L. Blackburn, T. M. Barnes, M. C. Beard, Y.-H. Kim, R. C. Tenent, T. J. McDonald, B. To, T. J. Coutts, M. J. Heben, *ACS Nano* **2008**, *2*, 1266.
[267] C. Niu, *MRS Bulletin* **2011**, *36*, 766.
[268] D. S. Hecht, R. B. Kaner, *MRS Bulletin* **2011**, *36*, 749.
[269] L. Hu, H. Wu, Y. Cui, *MRS Bulletin* **2011**, *36*, 760.
[270] M. G. Kang, L. J. Guo, *Adv. Mater.* **2007**, *19*, 1391.
[271] M. G. Kang, M. S. Kim, J. S. Kim, L. J. Guo, *Adv. Mater.* **2008**, *20*, 4408.
[272] S. Magdassi, M. Grouchko, D. Toker, A. Kamyshny, I. Balberg, O. Milo, *Langmuir* **2005**, *21*, 10264.
[273] M. Layani, M. Grouchko, O. Milo, I. Balberg, D. Azulay, S. Magdassi, *ACS Nano* **2009**, *3*, 3537.
[274] D. J. Harris, H. Hu, J. C. Conrad, J. A. Lewis, *Phys. Rev. Lett.* **2007**, *98*, 148301.
[275] I. U. Vakarelski, D. Y. Chan, T. Nonoguchi, H. Shinto, K. Higashitani, *Phys. Rev. Lett.* **2009**, *102*, 148301.
[276] K. Higashitani, C. E. McNamee, M. Nakayama, *Langmuir* **2011**, *27*, 2080.
[277] J.-Y. Lee, S. T. Connor, Y. Cui, P. Peumans, *Nano Lett.* **2008**, *8*, 689.
[278] W. Gaynor, J.-Y. Lee, P. Peumans, *ACS Nano* **2010**, *4*, 30.
[279] Z. Yu, Q. Zhang, L. Li, Q. Chen, X. Niu, J. Liu, Q. Pei, *Adv. Mater.* **2011**, *23*, 664.
[280] A. R. Madaria, A. Kumar, C. Zhou, *Nanotechnology* **2011**, 245201.
[281] V. Scardaci, R. Coull, P. E. Lyons, D. Rickard, J. N. Coleman, *Small* **2011**, *7*, 2621.

[282] L. Hu, H. S. Kim, J.-Y. Lee, P. Y. Cui, *ACS Nano* **2010**, *4*, 2955.
[283] C.-H. Liu, X. Yu, *Nanoscale Res. Lett.* **2011**, *6*, 75.
[284] D.-S. Leem, A. Edwards, M. Faist, J. Nelson, D. D. C. Bradley, J. C. de Mello, *Adv. Mater.* **2011**, *23*, 4371.
[285] M.-G. Kang, T. Xu, H. J. Park, X. Luo, L. J. Guo, *Adv. Mater.* **2010**, *22*, 4378.
[286] S. De, T. M. Higgins, P. E. Lyons, E. M. Doherty, P. N. Nirmalraj, W. J. Blau, J. J. Boland, J. N. Coleman, *ACS Nano* **2009**, *3*, 1767.
[287] J. Xu, C. Zhong, C. Fu, *SPIE Newsroom* December 26, **2007**, 10.1117/2.1200712.0969.
[288] L. Yang, T. Zhang, H. Zhou, S. C. Price, B. J. Wiley, W. You, *ACS Appl. Mater. Interfaces* **2011**, *3*, 4075.
[289] D. Azulay, T. Belenkova, H. Gilon, Z. Barkay, G. Markovich, *Nano Lett.* **2009**, *9*, 4246.
[290] A. R. Rathmell, S. M. Bergin, Y.-L. Hua, Z. Y. Li, B. J. Wiley, *Adv. Mater.* **2010**, *22*, 3558.
[291] A. R. Rathmell, B. J. Wiley, *Adv. Mater.* **2011**, *23*, 4798.
[292] A. R. Rathmell, M. Nguen, M. Chi, B. J. Wiley, *Nano Lett.* **2012**, *12*, 3193.
[293] H. Wu, L. Hu, M. W. Rowell, D. Kong, J. J. Cha, J. R. McDonough, J Zhu, Y. Yang, M. D. McDehee, Y. Cui, *Nano Lett.* **2010**, *10*, 4242.
[294] Cambrios silver nanowires to revolutionize touch screens and display. Available from: http://www.youtube.com/watch?v=TbtbM_C_J7I.
[295] H. C. Schniepp, J. L. Li, M. J. McAllister, H. Sai, M. Herrera-Alonso, D. H. Adamson, R. K. Prud'homme, R. Car, D. A. Saville, I. A. Aksay, *J. Phys. Chem. B* **2006**, *110*, 8535.
[296] C. Gómez-Navarro, T. R , Weitz, A. M. Bittner, M. Scolani, A. Mews, M. Burghard, K. Kern, *Nano Lett.* **2007**, *7*, 3499.
[297] X. Wang, L. Zhi, K. Müllen, *Nano Lett.* **2008**, *8*, 323.
[298] J. T. Robinson, M. Zalalutdinov, J. W. Baldwin, E. S. Snow, Z. Wei, P. Sheehan, B. H. Houston, *Nano Lett.* **2008**, *8*, 3441.
[299] H. A. Becerill, J. Mao, Z. Liu, R. M. Stoltenberg, Z. Bao, Y. Chen, *ACS Nano* **2008**, *2*, 463.
[300] S. Pang, H. N. Tsao, X. Feng, K. Müllen, *Adv. Mater.* **2009**, *21*, 3488.
[301] H. Yamaguchi, G. Eda, C. Mattevi, H. Kim, M. Chhowalla, *ACS Nano* **2010**, *4*, 524.
[302] Z. Yin, S. Sun, T. Salim, S. Wu, X. Huang, Q. He, Y. M. Lam, H. Zhang, *ACS Nano* **2010**, *4*, 5263.
[303] S. Gijie, S. Han, M. Wang, K. L. Wang, R. B. Kaner, *Nano Lett.* **2007**, *7*, 3394.
[304] Y. Chen, X. Zhang, P. Yu, Y. Ma, *Chem. Commun.* **2009**, 4527.
[305] V. Lee, L. Whittaker, C. Jaye, K. M. Baroudi, A. A. Fischer, S. Banerjee, *Chem. Mater.* **2009**, *21*, 3905.
[306] K.-Y. Shin, J.-Y. Hong, J. Jang, *Chem. Commun.* **2011**, *47*, 8527.
[307] T. V. Sreekumar, T. Liu, S. Kumar, L. M. Ericson, R. H. Hauge, R. E. Smalley, *Chem. Mater.* **2003**, *15*, 175.
[308] S. Pei, J. Du, Y. Zeng, C. Liu, H.-M. Cheng, *Nanotechnology* **2009**, *20*, 235707.
[309] A. J. Stapleton, R. A. Afre, A. V. Ellis, J. G. Shapter, G. G. Andersson, J. S. Quinton, D. A. Lewis, *Sci. Technol. Adv. Mater.* **2013**, *14*, 035004.
[310] C. M. Trottier, P. Glatkowski, P. Wallis, J. Luo, *J. Soc. Inf. Disp.* **2005**, *13/9*, 759.
[311] V. Subramanian, J. M. J. Fréchet, P. C. Chang, D. C. Huang, J. B. Lee, S. E. Molesa, A. R. Murphy, D. R. Redinger, S. K. Volkman, *IEEE Proc.* **2005**, *93*, 1330.
[312] Y. Noguchi, T. Sekitani, T. Yokota, T. Someya, *Appl. Phys. Lett.* **2008**, *93*, 043303.
[313] G. L. Whiting, A. C. Arias, *Appl. Phys. Lett.* **2009**, *95*, 253302.
[314] P. Chen, Y. Fu, R. Aminarad, C. Wang, J. Zhang, K. Wang, K. Galatsis, C. Zhou, *Nano Lett.* **2011**, *11*, 5301.
[315] S. Lim, B. Kang, D. Kwak, W. H. Lee, A. Lim, K. Cho, *J. Phys. Chem. C* **2012**, *116*, 7520.
[316] C. J. Curtis, A. Miedaner, T. Rivkin, J. Alleman, D. L. Schultz, D. S. Ginley, *Mater. Res. Soc. Symp. Proc.* **2000**, *624*, 59.

Received: September 16, 2013
Revised: November 13, 2013
Published online: January 25, 2014